Performance and Mechanism Analysis of Pb(II) Removal by Algal-bacterial Aerobic Granular Sludge

July 2023

Wang Zhiwei

Performance and Mechanism Analysis of Pb(II) Removal by Algal-bacterial Aerobic Granular Sludge

A Dissertation Submitted to
the Graduate School of Science and Technology,
University of Tsukuba
in Partial Fulfillment of Requirements
for the Degree of Doctor of Philosophy in Environmental Studies

Doctoral Program in Environmental Studies,
Degree Programs in Life and Earth Sciences

Wang Zhiwei

Abstract

Heavy metals (HMs) often discharge together with various types of wastewater, which become a big challenge to wastewater treatment plants (WWTPs) since the general wastewater treatment processes are not sufficient for the efficient removal of HMs. Among them, lead (Pb) receives wide concern due to its severe effects on human health. Large amounts of wastewater containing Pb(II) are discharged into the environment from many Pb-associated rural industries. If the Pb(II) accumulated aquatic organisms are processed as food for human consumption, it will cause irreversible damage to the human body.

Among many excellent methods for the treatment of wastewater containing relatively low Pb(II) concentrations, biosorption is regarded as an efficient and eco-friendly method. Aerobic granular sludge (AGS) is thought to be an alternative to the conventional activated sludge widely applied in WWTPs due to its high efficiency of nutrient removal and excellent settleability. Algal-bacterial AGS has been recently developed as a promising technology with enhanced performance for wastewater treatment. However, to the best of our knowledge, little information is now available for the treatment performance of Pb(II) containing wastewater using the algal-bacterial AGS, let alone the mechanisms involved in the biosorption process. Moreover, the recovery of adsorbed Pb(II) and the downstream process for Pb-loaded algal-bacterial AGS should also be considered to reduce the secondary environmental impacts and realize sustainable development.

In this context, this study attempted to analyze the Pb(II) biosorption performance using algal-bacterial AGS as well as reveal the involved mechanisms and Pb distribution in Pb-adsorbed algal-bacterial AGS. The main research findings can be summarized below:

The Pb(II) removal performance was analyzed with the influencing factors including pH, contact time, initial Pb(II) concentration, coexisting ion, and granular dosage being evaluated. Initial pH of 6.0 was determined as the optimal pH condition for Pb(II) biosorption by algal-bacterial AGS. The reaction equilibrium was achieved at about 24 h with the biosorption process better fitted the pseudo-second-order kinetic model. The biosorption isotherm better fitted the Langmuir isotherm model with a maximum adsorption capacity of 72.4 mg/g. Co-existing ions (Cr, Cu, Zn and Cd) slightly influenced Pb(II) removal by algal-bacterial AGS. When the granule dosage was 10 g/L, the Pb(II) concentration was 0.06 ± 0.02 mg/L which met the effluent discharge standard. Considering the quick cultivation, easy harvesting or separation, and excellent adsorption performance, the algal-bacterial AGS without pretreatment was proposed as a promising alternative to removing Pb(II) from wastewater.

Pb removal mechanisms were investigated with the role of EPS being analyzed. Both physicochemical and biological effects were involved in the biosorption process. Electrostatic interaction, ion exchange, and bonding to functional groups contributed to Pb(II) biosorption. EPS played an important role in keeping microbial activity, Pb bonding, and ion exchange in algal-bacterial AGS. Under the conditions of this experiment, 66% of the adsorbed Pb was found in the residue part (microbial cells or mineral particles) by bioaccumulation and the formation of pyromorphite precipitate ($Pb_5(PO_4)_3Cl$).

The Pb(II) distribution in Pb-loaded algal-bacterial AGS and the optimal desorption reagent were further studied. For the adsorbed Pb in algal-bacterial AGS, 61.3% and 3.1% of them were in the organic-bound or residue fractions while 22.6% were found in the mobile fraction. Over 60% of Pb was intracellularly immobilized but the proportion for Mg or Ca was 45%, implying that the metals located in the extracellular part of algal-bacterial AGS were more likely to be mobile forms. Na_2EDTA (0.05 mol/L) solution was determined as the optimal desorbent that could recover 60.3% of the loaded Pb from the algal-bacterial AGS.

All the findings from this study are expected to provide the theoretical reference for the application of algal-bacterial AGS for cost-effective remediation of Pb(II)-containing wastewater, contributing to mitigating the Pb-derived environmental pollution and health risk. Further studies are still required to provide an overall evaluation of algal-bacterial AGS for Pb(II)-containing wastewater treatment. These include but are not limited to in-depth Pb-containing wastewater characterization, the role of microorganisms in the Pb(II) biosorption process, cost-efficient volume reduction methods for Pb-loaded granules as well as the toxicity and ecological impacts of the treated wastewater and the generated algal-bacterial biomass. At the same time, the methods to keep the microbial activity and granular stability are also significant to investigate.

Keywords: Algal-bacterial aerobic granular sludge (AGS); Heavy metals (HMs); Pb(II); Extracellular polymeric substances (EPS); Biosorption; Desorption

Contents

List of tables

List of figures

Abbreviations

AGS	Aerobic granule sludge
Chl-*a*	Chlorophyll *a*
COD	Chemical oxygen demand
DO	Dissolved oxygen
DOC	Dissolved organic carbon
EPS	Extracellular polymeric substances
FT-IR	Fourier transform infrared
HMs	Heavy metals
ICP-AES	Inductively coupled plasma-Auger electron spectroscopy
LB-EPS	Loosely bound EPS
MF	Mobility factor
MLSS	Mixed liquor suspended solids
MLVSS	Mixed liquor volatile suspended solids
NOMs	Natural organic matters
PN	Proteins
PS	Polysaccharides
SBR	Sequencing batch reactor
SEM	Scanning electron microscope
S-EPS	Soluble EPS
SVI	Sludge volume index
TB-EPS	Tightly bound EPS
TOC	Total organic carbon
TP	Total phosphorus
TN	Total nitrogen
TS	Total solids
VSS	Volatile suspended solids
WWTP	Wastewater treatment plant

WAS	Waste activated sludge
XPS	X-ray photoelectron spectroscopy
XRD	X-ray diffractometer

Chapter 1 Introduction

1.1. Heavy metals issue and Lead

Heavy metals (HMs), including lead, are a significant concern due to their toxic effects on human health and the environment (Jaishankar et al., 2014). The hypergrowth of living standards drives the prosperity of metal industries like mining, metallurgy, electroplating, and so forth (Abu-Danso et al., 2018). In this context, some HMs-containing wastewater is inevitably discharged into the aquatic ecosystem, causing heavy metal pollution in soils and plants (Tan et al., 2022). HMs are usually harmful and non-biodegradable, which poses a significant safety risk to the environment and humans, leading to one of the most prominent environmental concerns (Wang et al., 2022c). Among many HMs, lead (Pb) should be concerned more due to its widespread use in the lead-acid battery, cable, the chemical industry, etc., owing to its excellent physicochemical properties like outstanding conductibility and good corrosion resistance, etc. Its pollution in the aquatic ecosystem should be paid particular attention to since it can be easily transferred through the food chain into the human body. Even at a very low concentration in water, Pb can be bioaccumulated in organisms, causing severe diseases in the human, like anemia, enteric dysbacteriosis, and even death (Zeng et al., 2020; Zeng et al., 2022). In this context, Pb is listed as the second most toxic HM, and many countries have introduced policies to limit Pb(II) concentration in water (Cheng et al., 2022). Efforts to reduce lead exposure have significantly improved public health outcomes, but challenges remain, especially in older buildings, industrial settings, and certain geographic regions. Ongoing monitoring, enforcement of regulations, and continued public awareness are vital to further mitigate the risks associated with lead exposure and protect human health.

1.2. Removal methods for Lead

Although the wastewaters usually contain a relatively low Pb(II) concentration of 3.50-35.94 mg/L, it is still higher than the maximum concentration (0.1 mg/L) of effluent discharge standard set by the World Health Organization (WHO) (WHO, 2021; Liao et al., 2021; Xi et al., 2019). If the Pb(II) contained aquatic organisms are processed as food for human consumption, it will cause irreversible damage to the human body by inducing anaemia, neurological disorders and even death (Zeng et al., 2020). In China, the amount of Pb(II) discharged into the water environment increased from 51.38 tons in 2014 to 71.78 tons in 2016

(Wang et al., 2019).

When it comes to the removal of Pb from wastewater, several methods like adsorption, precipitation, membrane filtration, electrodialysis, and others can be employed. Here are some commonly used methods (Table 1-1) along with their advantages and disadvantages (Fu and Wang, 2011):

(1) Ion exchange

- Advantages: Ion exchange is a highly effective method for removing HMs, including Pb, from wastewater. It involves exchanging Pb ions with less toxic ions on the resin surface. The process can achieve high removal efficiencies and can be used for both batch and continuous operations.

- Disadvantages: Ion exchange resins may need to be regenerated or replaced periodically, which increases the operational costs. The regeneration process involves the use of chemicals, which must be properly managed (Gu et al., 2001). Disposal of spent resin can also be a concern.

(2) Chemical precipitation

- Advantages: Chemical precipitation methods, such as coagulation and flocculation, can effectively remove Pb from wastewater by forming insoluble precipitates (Fu and Wang, 2011). These methods are widely used and can achieve high removal efficiencies.

- Disadvantages: Chemical precipitation requires the addition of chemicals, such as coagulants or flocculants, which increase the overall cost. Proper monitoring and control are necessary to optimize the dosage and ensure efficient removal. Generated sludge requires proper disposal or treatment.

(3) Membrane filtration

- Advantages: Membrane filtration, including techniques like reverse osmosis or nanofiltration, can effectively remove lead and other contaminants from wastewater (Xiang et al., 2022). These methods provide a physical barrier to separate dissolved substances, allowing the production of treated water with high quality.

- Disadvantages: Membrane filtration can be energy-intensive and may require proper pre-treatment to avoid fouling or clogging of the membranes. The concentrate or brine generated during the process needs proper management. The high-pressure requirements of reverse osmosis contribute to the high operational costs.

(4) Electrolysis

- Advantages: Electrolysis methods, such as electrocoagulation or electrochemical precipitation, can effectively remove Pb from wastewater. These methods use electricity to generate coagulating agents or induce precipitation, facilitating the removal of Pb and other contaminants (Bazrafshan et al., 2015).

- Disadvantages: Electrolysis treatment can be energy-intensive, particularly for large-scale applications. Electrodes may require periodic maintenance or replacement. Generated sludge or byproducts may require proper handling and disposal.

(5) Biological treatment

- Advantages: Some microorganisms, such as sulfate-reducing bacteria, can aid in the removal of lead from wastewater through biological processes. Biological treatment can be cost-effective and environmentally friendly (Xu and Chen, 2020).

- Disadvantages: Biological treatment may have limitations in terms of lead removal efficiency and applicability to specific wastewater streams. It requires careful control of operating conditions, including pH, temperature, and nutrient levels. The process may have a longer treatment time compared to some other methods.

(6) Adsorption

- Advantages: Adsorption methods, such as activated carbon or other adsorbents, can effectively remove Pb from wastewater. Activated carbon is a commonly used adsorbent due to its high adsorption capacity and versatility. Adsorption can be employed in both batch and continuous systems (Goel et al., 2005).

- Disadvantages: Adsorption may require a significant contact time for effective removal, and the efficiency can be influenced by the presence of other contaminants in the wastewater. Regeneration or replacement of adsorbents can be necessary, adding to the overall cost.

It is important to note that different methods may have advantages and limitations depending on the specific circumstances. Selection of the appropriate Pb removal method should consider factors such as the effectiveness of removal, cost, feasibility, and environmental considerations. At the same time, since the Pb(II) concentrations in real industrial wastewater or waste acid are relatively low (3.50-35.94 mg/L), adsorption could be a better choice for its relatively lower price and higher efficiency (Liao et al., 2021; Xi et al., 2019).

1.3. Biosorption and biosorbents

Biosorption is a process that contaminants including organic pollutants or toxic heavy metals are concentrated on the surface of biosorbents from solutions. The biosorption process for Pb(II)-containing wastewater has become a promising technology due to its high efficiency and low operating costs (Fu and Wang, 2011). Among the various types of adsorbents, biosorbents have received increasing attention in recent years due to their abundant sources, low cost, and various types of available active sites provided by the unique characteristics of cell membranes and organic materials (Qin et al., 2020). These biosorbents can be obtained

from live or dead fungi (Xu et al., 2020b), bacteria (Zhang et al., 2020b), algae (Kipigroch, 2020), yeast (Amirnia et al., 2015), agricultural and forest wastes (Das et al., 2020; Kim et al., 2015), activated sludge (Taki et al., 2019), and bacterial aerobic granular sludge (AGS) (Xu et al., 2020a). As by-product of wastewater treatment plants (WWTP), waste activated sludge (WAS) is cost-effective and has been proven to be efficient in HMs removal (Wu et al., 2010). Utilization of WAS for HMs treatment could reduce disposal issues and remove hazardous pollutants simultaneously. The main components in waste WAS are polysaccharides, proteins and lipids with various functional groups for the binding of metal ions (Zhou et al., 2016). However, biomass of WAS in the form of suspended flocs with poor settling ability results in high energy requirement in the post-separation process when applied for HMs removal. Moreover, freely suspended microbial cells in WAS can easily be disintegrated under high pressures and loss its efficiency, thus limiting its industrial applications.

Fortunately, a new technology of AGS can overcome some limitations of WAS, due to the many superior properties of AGS like porous microbial structure, excellent settleability, rich binding sites for metals and the ability to withstand shock and toxicant loadings (Franca et al., 2018). Up to now, original or surface-modified AGS has been proven to be highly effective towards various heavy metals. However, the drawbacks of the AGS process, like the relatively low structural stability during prolonged operations, and the slow growth of AGS biomass, limit the biosorbent development from the AGS process (Yang et al., 2020).

1.4. Algal-bacterial AGS

Recently, algal-bacterial AGS, a novel type of AGS, is widely studied. Algae can naturally grow on AGS and entangle with bacterial biomass rapidly when exposed to artificial sunlight (Zhang et al., 2018). This kind of granular consortium of algae and bacteria can be quickly established due to fast algal biomass growth, which also exhibited an excellent and stable nutrient removal performance after maturation. It involves the symbiotic growth of both algae and bacteria within a gel-like matrix, forming compact granules with unique characteristics. Here are some key features and benefits of algal-bacterial AGS:

(1) Enhanced nutrient removal: The combination of algae and bacteria in the granules allows for the simultaneous removal of various nutrients from wastewater, including nitrogen and phosphorus (Dong et al., 2021). Algae utilize dissolved nutrients for growth, while bacteria degrade organic matter and convert ammonia to nitrate through nitrification.

(2) High biomass concentration: Algal-bacterial AGS can achieve high biomass concentrations, which results in more efficient treatment processes (Zhang et al., 2018). The compact structure

of the granules allows for higher microbial densities, increasing the overall treatment capacity within a smaller footprint.

(3) Improved settling and separation: The granular structure of the sludge enhances settling properties, facilitating the separation of treated water from biomass (Zhang et al., 2018). This characteristic helps improve the overall solids-liquid separation process, resulting in clearer effluent quality and high-efficient treatment.

(4) Resistance to toxic substances: Algal-bacterial AGS have been found to exhibit enhanced resistance to toxic substances, such as HMs and certain organic pollutants (Zhang et al., 2020a). The combined action of algae and bacteria can effectively degrade or sequester these contaminants, contributing to the detoxification of wastewater.

(5) Algal oxygen supply: Algae in the granules produce oxygen through photosynthesis, which can enhance the oxygen availability for aerobic bacteria within the sludge (Meng et al., 2019). This promotes the growth of aerobic bacteria, improving the overall treatment efficiency and reducing the need for external aeration.

(6) Energy efficiency: Algal-bacterial AGS systems have the potential for energy savings compared to traditional wastewater treatment methods. The photosynthetic activity of algae reduces the demand for external energy input for aeration, which is typically required in conventional activated sludge systems (Saravanan et al., 2021).

(7) Potential resource recovery: Algal-bacterial granules offer the opportunity for resource recovery from wastewater. The biomass produced in the process can be further utilized as a source of bioenergy, such as for biogas generation, or as a valuable nutrient-rich fertilizer (Zhang et al., 2020a).

While algal-bacterial AGS shows promise in wastewater treatment, further research and optimization are still needed to refine the technology and maximize its efficiency. Factors such as granular formation and stability, control of algal-bacterial interactions, and operational parameters need to be carefully managed to ensure consistent and reliable performance in different wastewater treatment scenarios. At the same time, algae has fast biomass growth, which can effectively adsorb HMs from wastewater due to its large surface-to-volume ratio (Kumar et al., 2015) and high selectivity of specific heavy metals binding (Son et al., 2018).

1.5. Application of algal-bacterial AGS for heavy metals removal

1.5.1. Main pathways and advantages

Algal-bacterial AGS systems have shown great promise for the removal of HMs from various wastewater sources (Yang et al., 2020; Zhang et al., 2019). Algal-bacterial AGS integrates algae and bacteria in AGS, which offers several advantages for HMs removal, including high adsorption capacity, resilience to environmental fluctuations, and the potential for metal recovery. The main pathways involved in algal-bacterial AGS and its advantages for HMs removal were summarized as below:

(1) Biosorption: Algae and bacteria in AGS have the ability to adsorb HM ions onto their cell surfaces. Algal cells, in particular, have a high affinity for HMs due to their negatively charged cell walls and various functional groups (Zhao et al., 2023). Bacterial EPS also contribute to metal binding (Wei et al., 2017), making the algal-bacterial AGS system highly effective in removing HMs from wastewater.

(2) Metal precipitation: Algae and bacteria can facilitate the precipitation of HMs in the algal-bacterial AGS system through biologically induced mineralization (Zhang et al., 2020a). This process involves the conversion of metal ions into less soluble forms, reducing their bioavailability and enhancing their removal from the water phase.

(3) Cellular accumulation: The ability of algae to bioaccumulate HMs within their cells is utilized in algal-bacterial AGS systems (Yang et al., 2021a). As algae grow and multiply, HMs are concentrated within their biomass, which can then be harvested for metal recovery or safe disposal.

(4) Synergistic microbial activity: The coexistence of algae and bacteria in algal-bacterial AGS creates a mutualistic relationship. Algae produce oxygen through photosynthesis, providing aerobic conditions that promote the growth and activity of metal-reducing bacteria (Meng et al., 2019). This synergy enhances the overall efficiency of HMs removal.

(5) Nutrient uptake and competition: The presence of algae in algal-bacterial AGS can promote the uptake of essential nutrients like phosphorus and nitrogen, which may otherwise facilitate the growth of undesirable microorganisms (Xiong et al., 2023). This nutrient competition can suppress the growth of certain bacteria that contribute to the release of HMs back into the water (Ilmasari et al., 2022).

(5) Continuous operation and stability: Algal-bacterial AGS systems are known for their stability and robustness, allowing for continuous operation even under varying influent conditions (Zhang et al., 2020a). This makes them suitable for treating wastewater with fluctuating HM concentrations.

(6) Metal recovery and reuse: One of the significant advantages of algal-bacterial AGS is the potential for metal recovery (Zhao et al., 2023). After HMs accumulated in the biomass, the

harvested algae and bacteria can be processed to extract valuable metals for recycling or other industrial applications.

However, despite the numerous advantages, challenges remain, including the need for further optimization, understanding the dynamics of HMs interaction within the algal-bacterial AGS system, and the potential release of HMs under certain conditions. Continued research and development will contribute to maximizing the potential of algal-bacterial AGS for effective and sustainable HMs removal in wastewater treatment.

1.5.2. Influencing factors

The performance of algal-bacterial AGS for HMs removal depends on several factors, including the specific HMs present, their concentrations in the wastewater, the composition of the algal-bacterial consortia, and the operational conditions of the treatment system (Zhao et al., 2023). Here are some considerations regarding the performance of algal-bacterial AGS for HMs removal:

(1) Metal-specific affinity: Different heavy metals exhibit varying affinities for biosorption by algae and bacteria. Some heavy metals, such as copper (Cu), zinc (Zn), and nickel (Ni), have a higher affinity for biosorption by algal surfaces, while others like cadmium (Cd), lead (Pb), and chromium (Cr) tend to be more readily adsorbed by bacterial cells. The composition of the algal-bacterial consortia and the relative proportions of algae and bacteria can influence the overall heavy metal removal efficiency (Zhao et al., 2023).

(2) Concentration and loading rate: The concentration of heavy metals in the wastewater and the loading rate (the amount of metal ions entering the system per unit time) can impact the performance of algal-bacterial granules (Priyadharshini et al., 2021). Higher concentrations and loading rates may saturate the biosorption capacity of the granules, resulting in decreased removal efficiency (Goel et al., 2005). Therefore, the design and operation of the system should consider the metal concentration and loading rate to ensure optimal performance.

(3) Granular characteristics: The characteristics of the algal-bacterial granules, such as their size, density, and stability, can affect heavy metal removal performance. Larger and denser granules tend to have better settling properties, leading to improved separation of the biomass from the treated water (Franca et al., 2018). Granular stability is crucial to maintain the integrity of the microbial consortia and prevent disintegration or washout of the granules, which could result in reduced metal removal efficiency.

(4) Nutrient availability: Adequate nutrient availability, particularly nitrogen and phosphorus, is essential for the growth and metabolism of algae and bacteria in the granules. Insufficient

nutrient supply can limit biomass growth and metabolic activities, potentially affecting heavy metal removal performance (Zhang et al., 2020a). Optimization of nutrient dosing and monitoring is necessary to ensure optimal performance.

(5) Operational conditions: The operational conditions of the treatment system, including temperature, pH, and hydraulic retention time, can influence HMs removal performance. Some HMs exhibit higher removal efficiency under specific pH ranges or temperature conditions (Sanchez-Sanchez et al., 2023). The hydraulic retention time should be sufficient to allow the algal-bacterial granules to come into contact with the heavy metal-contaminated wastewater for effective removal.

(6) Presence of co-contaminants: The presence of co-contaminants, such as organic matter or other inorganic substances, in the wastewater can affect heavy metal removal performance (Yuan et al., 2023). Competitive adsorption or complexation reactions may occur, which could hinder the biosorption or precipitation of heavy metals. Understanding the composition and characteristics of the wastewater is important to evaluate the overall performance of the algal-bacterial granule system.

It is worth noting that the performance of algal-bacterial AGS for HMs removal is still an active area of research, and the specific performance outcomes may vary depending on the system design, microbial consortia composition, and wastewater characteristics. Continuous monitoring and optimization of the system are necessary to achieve consistent and effective HMs removal.

1.6. Problems statement

At present, AGS has been widely used in domestic wastewater treatment for nitrogen removal and phosphorus recovery. Previous study showed that algal-bacterial AGS exhibits better performance for some HMs removal (Yang et al., 2020). However, the removal performance of algal-bacterial AGS for Pb(II) is remain unknown, let alone the involved mechanisms.

In addition, the influencing factors for Pb(II) adsorption performance by algal-bacterial AGS need to be explored. Further, Pb(II) distribution in the granules and desorption methods to recover adsorbed Pb on granules should be evaluated to provide important information for practical application and sustainable treatment.

1.7. Research objectives and novelty

As mentioned above, algal-bacterial AGS is a promising biosorbent for HMs removal. At the same time, little information is now available for Pb(II) removal by algal-bacterial AGS, let alone the involved mechanisms and potential application for real wastewater treatment. In this context, the objectives of this study are as follows: 1) to analyze the Pb(II) biosorption performance using algal-bacterial AGS by considering typical influencing factors; 2) to reveal the involved mechanisms especially the role of extracellular polymeric substances (EPS) and the physicochemical properties of granules; 3) to clarify the Pb distribution and desorption from Pb-adsorbed algal-bacterial AGS. Results from the study are expected to provide the theoretical basis for the practical application of algal-bacterial AGS for cost-effective bioremediation of Pb(II)-containing wastewater, contributing to mitigating the Pb-derived environmental pollution and health risk.

1.8. Thesis structure and main content

The structure (Figure 1-1) and main content of this thesis were summarized below:

Chapter 1 gave an overview of HMs issues, and introduced typical removal methods for Pb(II). The advantages and disadvantages of each method were summarized and biosorption was proposed as a preferable method for HMs removal. Then, the advantages and previous reports on HMs removal using algal-bacterial AGS were summarized. In addition, the involved pathway and influencing factors were addressed. Finally, the problems statement and objectives of this study were pointed out.

Chapter 2 clarified the adsorption performance of algal-bacterial AGS on the Pb(II) removal with 5 typical parameters being analyzed, including pH, contact time and initial Pb(II) concentration, coexisting ion and granular dosage.

Chapter 3 mainly revealed the biosorption mechanism with special focus on the role of EPS. The variation of protein (PN), polysaccharide (PS) and metal ions in EPS were analyzed. The physical and chemical properties of the algal-bacterial AGS were analyzed.

Chapter 4 analyzed the metal distribution and Pb(II) desorption method from Pb-loaded algal-bacterial AGS. The proportion of different metal forms and intra/extracellular distribution of metals were determined. Chemical desorption methods with different types of chemicals and concentrations were evaluated.

Chapter 5 summarized the research findings in the present research. For the application of algal-bacterial AGS to bioremediate Pb(II)-containing wastewater, future research perspectives are proposed.

Table 1-1 Comparison of treatment technologies for heavy metals (HMs)-containing wastewater.

Methods	**Advantages**	**Disadvantages**	**Reference**
Ion exchange	1) High treatment capacity 2) High removal efficiency	1) High cost 2) Serious secondary pollution	Ahmed et al. (1998)
Chemical/Physical precipitation	1) Simple operation 2) Low cost	1) Extra operational cost for sludge disposal 2) Can't treat wastewater with low concentration	Vardhan et al. (2019)
Membrane filtration	1) High separation selectivity 2) Small space requirement 3) Low-pressure requirement	1) High cost 2) Process complexity 3) Low processing rate	Chadha et al. (2022)
Electrolysis	1) High separation selectivity	1) High cost	Li et al. (2017b)
Biological treatment	1) Cost-effective 2) Environmentally friendly	1) Exacting operating conditions 2) Low processing rate	Hoa et al. (2007) Zhang et al. (2016)
Adsorption/Biosorption	1) Design flexibility 2) High efficiency 3) Low cost	1) Produce waste products 2) Low selectivity	Abbas et al. (2014)

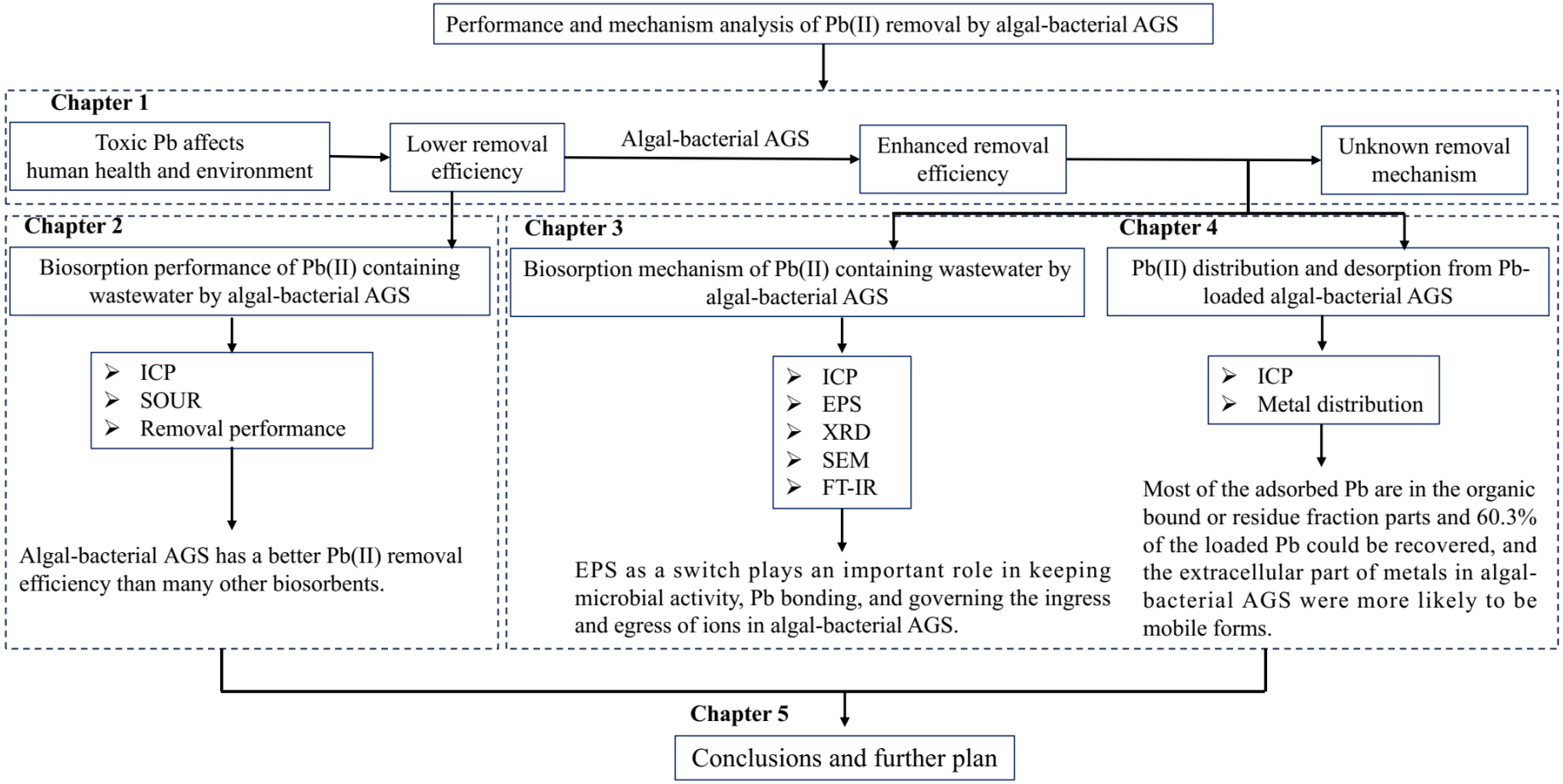

Figure 1-1. The research framework of this thesis.

Chapter 2 Biosorption performance of Pb(II) containing wastewater by algal-bacterial aerobic granular sludge

2.1. Introduction

Pb(II) in wastewater can be removed by many techniques including ion exchange, precipitation, membrane filtration, electrodialysis and adsorption. biosorption can be a better choice when considering operation cost, environmental friendliness, and relatively low Pb(II) concentration in industrial wastewater (Lyu et al., 2021). Algal-bacterial AGS was reported to have better performance than bacterial AGS for removing oxyanion of Cr(VI), namely $Cr_2O_7^{2-}$, and microbial viability and algal participation contributed to this process were found to be mainly mediated by intracellular pathways (Yang et al., 2021a; Yang et al., 2020). However, few studies revealed the biosorption performance of Pb(II) using algal-bacterial AGS.

To bridge the above knowledge gap, this chapter investigated the adsorption performance of algal-bacterial AGS for Pb(II) removal from wastewater with the effect of pH (2.0-12.0), contact time (*t*, 0-24 h) and initial Pb(II) concentration ($C_{Pb(II)}$, 10-300 mg/L), coexisting ion (Cr, Cu, Zn and Cd, 5-100 mg/L) and dosage (0.2-10 g/L-MLSS) being analyzed.

2.2. Materials and methods

2.2.1. Cultivation of algal-bacterial AGS

In this study, algal-bacterial AGS was cultivated in a lab-scale sequencing batch reactor (SBR; H × D = 51 cm × 6 cm) with a working volume of 1 L. The SBR was first inoculated with mature bacterial AGS cultivated from activated sludge in a lab-scale reactor. As shown in Table 2-1, the synthetic domestic wastewater was used for the cultivation of algal-bacterial AGS with the main compositions of NH_4Cl (50 mg-N/L), CH_3COONa (300 mg-COD/L) and 1 mL/L of trace metals solution (Yang et al., 2020). The SBR was operated at room temperature (25±2 ℃) with a typical operation cycle of 6 h and an exchange ratio of 50%, resulting in a hydraulic retention time (HRT) of 12 h. Each cycle included 15-min feeding, 90-min non-aeration, 251-min aeration, 2-min settling, and 2-min effluent discharge. Artificial light with an illuminance of 3,000 lux was applied continuously (24 h/day) from the sidewall of the reactor to promote the formation of algal-bacterial AGS. After 14 days' cultivation, algal-bacterial AGS covered with algal with an average size of 2.05 mm (Figure 2-1) was harvested and used for the subsequent adsorption experiments. The detailed characteristics of the cultivated algal-bacterial AGS are shown in Table 2-2.

2.2.2. Batch Pb(II) biosorption on algal-bacterial AGS

The biosorption experiments were conducted at 25±1 ºC in 200 mL Erlenmeyer flasks with a working volume of 120 mL placed in a thermostatic rotary shaker with a shaking speed of 100 gravity. $Pb(NO_3)_2$ was chosen as the Pb(II) source due to the lower tendency of nitrate to form metal ion complexes (Yang et al., 2020). The Pb(II) stock solution with a concentration of 1,000 mg/L was prepared by dissolving 1.5986 g $Pb(NO_3)_2$ in 10 mL of 0.2% HNO_3 aqueous solution to prevent precipitation and diluted to 1 L using deionized water. Then, a certain amount of the prepared stock solution was diluted to the designated concentrations by serial dilution for the biosorption experiments. The solution pH monitored by pH meter (Mettler Toledo FE20 model) was adjusted to the designated values using 1 M HNO_3 or NaOH. The effects of pH (2.0-12.0), contact time (*t*, 0-72 h) and initial Pb(II) concentration ($C_{Pb(II)}$, 10-300 mg/L) (Liu et al., 2019; Liu et al., 2022), co-existing ion (Cr, Cu, Zn, Cd), different granular dosage (0.2-10 g-MLSS/L) on biosorption using algal-bacterial AGS were investigated. The dosage of algal-bacterial AGS (no further pretreatment after being sampled from the SBR reactor) was fixed at 1 g-MLSS/L. To investigate the effect of pH, the solutions with an initial Pb(II) concentration of 50 mg/L were used and the biosorption process lasted for 24 h. Adsorption kinetic experiments were carried out at predetermined intervals of time at pH 6.0 and 50 mg/L Pb(II). Adsorption isotherm experiments were carried out at different initial Pb(II) concentrations at pH 6.0 for 24 h. Effect of co-existing ion (Cr, Cu, Zn, Cd) on Pb(II) adsorption by algal-bacterial AGS was carried out at different concentrations (5, 10, 20, 50 and 100 mg/L) of each ion. The effect of granular dosage experiments on the Pb(II) removal by algal-bacterial AGS were carried out at different granular dosages (0.2-10 g-MLSS/L). After the biosorption experiments, 5 mL of supernatant liquid was sampled by syringe and filtrated through a 0.22 μm syringe-type membrane filter. Then, the filtrate sample (2 mL) was digested with 1 mL of concentrated HNO_3 (65%) and 1 mL of H_2O_2 (30%) at 100 ºC for 2 h to remove organic matters for the determination of Pb concentration (Yang et al., 2020). All the solutions were prepared or diluted using deionized water if there was no specific description.

2.2.3. Analytical methods

The MLSS, MLVSS and SVI_5 of the obtained algal-bacterial AGS were determined according to the standard methods (APHA, 2012). The morphology and size of algal-bacterial AGS were observed and measured using a Leica microscope (Leica M205C model). Inductively coupled plasma atomic emission spectroscopy (ICP-AES, ICP-8100 model) was used to analyze the metal ion concentration before and after biosorption. The pH was monitored by a pH meter (Mettler Toledo FE20 model). Dissolved oxygen (DO) and specific oxygen uptake rate (SOUR) were tested using a DO detector (HACH Hd40 model).

(1) Chlorophyll *a*

The Chlorophyll *a* (Chl-*a*) in algal-bacterial AGS was analyzed according to a previous study (Wang et al., 2022b). In brief, 5 mL of evenly crushed mixture in 15 ml centrifuge was centrifuged at 3,500 rpm for 15 min by a glass homogenizer (Sansyo, Japan) and the residue was resuspended in 10 mL of 90% methanol containing $MgCl_2$ solution. Then the mixture was heated at 70 °C for 30 min in the dark for extraction. Later, centrifugation was performed at 3,500 g for 10 min to separate the supernatant after being cooled down to room temperature, with the absorbance being recorded at the wavelengths of 750, 665, 645, and 630 nm, respectively using the UV–Visible spectrophotometer (UV 1800, Shimadzu, Japan). Chl-*a* concentration in the separated supernatant can be calculated according to Eq. (2-1).

$$\text{Chl-}a\ (\text{mg/L}) = [11.6\times(A_{665}-A_{750}) - 1.31\times(A_{645}-A_{750}) - 0.14\times(A_{630}-A_{750})]\times\frac{V_m}{V_f} \quad (2\text{-}1)$$

where V_m (mL) and V_f (mL) are the volumes of the extract methanol and the sample, respectively. Chl-*a* content (mg/g-MLSS) in microalgal was obtained by dividing Chl-*a* concentration (mg/L) by MLVSS (g/L) of the corresponding sample.

(2) Specific oxygen uptake rate (SOUR) and granular stability

The granular microbial activity indicated by SOUR and granular stability indicated by integrity coefficient before and after Pb biosorption were determined according to the previous studies (Yang et al., 2020). In brief, for the SOUR test, 3 g-wet weight (0.04 g-MLSS/g) granules were added into a 100 mL glass flask containing 90 mL synthetic wastewater (for algal-bacterial AGS cultivation), then an aerator and a dissolved oxygen (DO) meter (DO-31P, TOA-DKK, Japan) were inserted. The granular mixture was agitated with a magnetic stirrer at 300 rpm to ensure the suspension of granules when no aeration was supplied. The mixture was firstly aerated till a relatively stable DO level was achieved (over 5 mg-DO/L), then the aeration was stopped and at the same time, the flask was sealed with a DO meter inside. Due to the consumption of DO by microorganisms, the DO level decreased immediately and timely was recorded as DO_t. Then a DO versus time curve was made and only the linear portion was used for SOUR (mg-DO/(g-MLSS·h)) calculation with the equation: $SOUR = (DO_t\text{-}DO_1)/(t\cdot MLSS)$, in which DO_{t1} and DO_{t2} represented the DO value before and after the time interval (t), respectively. As for the testing of granular stability, 1 g wet-weight granules were added into a 50 mL plastic tube containing 40 mL DW. The mixture was firstly shaken at 200 rpm on a shaker for 5 min and then settled down for 1 min, the ratio of MLSS in the supernatant (30 mL) to the MLSS of total granules was recorded as the integrity coefficient.

2. 3. Data analysis

All the experiments were conducted in duplicate, and the samples were analyzed in triplicate with the results being expressed as means or mean ± standard deviation (SD). The calculation methods for the adsorption amount, adsorption kinetics, and adsorption isotherms

are as below. Significant differences in the results were assessed using *t*-test. All figures were plotted using Origin 2019.

2.3.1. Pb(II) adsorption amount

The Pb(II) adsorption amount of algal-bacterial AGS was calculated by Eq. (2-2) :

$$q = \frac{(c_0 - c_t)V}{m} \quad (2\text{-}2)$$

where q (mg/g-MLSS) is the Pb(II) adsorption amount of algal-bacterial AGS; c_0 (mg/L) and c_t (mg/L) are the Pb(II) concentrations at sampling time 0 and t (min), respectively; V (L) is the volume of the treated solution; m (g-MLSS) is the mass of the algal-bacterial AGS used in the test.

2.3.2. Adsorption kinetics

For analyzing the adsorption kinetics, the experimental data were fitted to the pseudo-first-order and pseudo-second-order models using Eqs. (2-3) and (2-4) (Nicomel et al., 2020),

$$q_t = q_e\left(1 - e^{(-k_1 t)}\right) \quad (2\text{-}3)$$

$$q_t = \frac{k_2 q_e^2 t}{1 + k_2 q_e t} \quad (2\text{-}4)$$

where q_t (mg/g-MLSS) is the Pb(II) adsorption amount of algal-bacterial AGS at contact time t (min); q_e (mg/g-MLSS) is the equilibrium adsorption capacity; k_1 (/min) and k_2 (g/mg/min) are the rate constants of the pseudo-first-order and pseudo-second-order kinetic models, respectively.

2.3.3. Adsorption isotherms

For analyzing the adsorption isotherms, the experimental data were fitted to the Langmuir and Freundlich isotherm models as described in Eqs. (2-5) and (2-6) (Fiol et al., 2006),

$$q_e = \frac{q_m K_L C_e}{1 + K_L C_e} \quad (2\text{-}5)$$

$$q_e = K_F C_e^{1/n} \quad (2\text{-}6)$$

where q_e (mg/g-MLSS) and q_m (mg/g-MLSS) are the equilibrium adsorption capacity and theoretical maximum adsorption capacity, respectively; K_L (L/mg) and K_F ((m/g)/(L/mg)$^{1/n}$) are the Langmuir and Freundlich constants, respectively; and 1/n is a dimensionless parameter.

2.4. Results and discussion

2.4.1. Effect of pH on Pb(II) removal

Solution pH can largely affect the chemical speciation of metal ions and the surface charge of biosorbents, which will eventually impact the removal performance of target pollutants from water (Ahmed et al., 2021). Therefore, the effect of initial solution pH (2.0-12.0) on Pb(II) biosorption was firstly investigated and the results are presented in Figure 2-2. Under acidic conditions (pH ≤ 6.0), Pb mostly exists as Pb^{2+} ion in the water, while at pH > 6.0, and the Pb would be easily hydrolyzed to form complex ions like $Pb_2(OH)_3^+$, $Pb_3(OH)_4^{2+}$, etc. to varying degrees (0-99.57%) at different pH (Figure 2-3), which will affect the determination of adsorption capacity of biosorbents (Wang et al., 2015). As shown in Figure 2-2, with the increase of initial pH, the Pb(II) concentration after biosorption decreased from 49.92 ± 0.32 mg/L at pH 2.0 to 40.01 ± 0.41 mg/L at pH 6.0 and then increased to 41.05 ± 0.42 mg/L at pH 12.0. The corresponding biosorption amount increased from 0.68 ± 0.22 mg/g to 12.30 ± 0.39 mg/g and then decreased to 8.5 ± 0.32 mg/g, and the removal efficiency increased from 1.4% to 24.6% and then decreased to 0.6%. The higher H^+ concentration at a lower pH in the solution can increase the surface charge of algal-bacterial AGS and create electrostatic repulsion, which could compete with the adsorption of Pb(II) on algal-bacterial AGS (Li et al., 2019), probably resulting in the lower biosorption amount at lower pH conditions. When the initial pH was increased from 2.0 to 6.0 and then to 12.0, the H^+ concentration in the solution will decrease sharply, which would weaken the competitive effect and significantly increase the adsorption sites, thus resulting in higher Pb(II) biosorption capacity of algal-bacterial AGS. Some more Pb precipitation like may form when pH ≥ 7 and the released ions (Na, Mg and Ca) are not analyzed when pH ≥ 7. Besides, at the initial pH of 2.0, higher concentrations of main metal ions including Na, Mg and Ca in algal-bacterial AGS were released into the bulk solution (Figure 2-4). The higher H^+ concentration at acidic pH of 2.0-4.0 might negatively impact the structure, extracellular polymeric substances (EPS) and microbial viability of algal-bacterial AGS, probably resulting in the release of these cations. Since EPS and microbial viability play important roles in heavy metal removal (Yang et al., 2020), the Pb(II) biosorption capacity of algal-bacterial AGS significantly declined at the initial solution pH of 2.0-4.0. Thus, initial pH of 6.0 was determined as the optimal pH condition for Pb(II) biosorption in the following biosorption experiments.

2.4.2. Biosorption kinetics

Contact time is one of the important factors for adsorption performance (Yetis et al., 2000). Therefore, the effect of contact time on Pb biosorption using algal-bacterial AGS was investigated. Figure 2-5 shows the variations of Pb(II) concentration ($C_{Pb(II)}$) during the adsorption and biosorption amount (q) of algal-bacterial AGS along with the contact time (t, 0-72 h) with the 3 stages divided according to the adsorption rate. It can be seen that the Pb(II)

concentration in the solution continuously decreased from 50 mg/L to 39 mg/L with the increase of contact time from 0 to 72 h. The biosorption process can be divided into three stages according to the adsorption rate. In the first stage, Pb(II) concentration rapidly decreased from 0 to 2 h since the numerous active sites are available on the surface of algal-bacterial AGS, which can provide attachment sites for Pb(II). Moderate adsorption occurred in the second stage from 2 h to 24 h, during which the adsorption rate was decreased compared to the first stage due to the reduced active sites on algal-bacterial AGS. In the third stage from 24 h to 72 h, the adsorption rate became extremely slow. As shown in Figure 2-6, with the Pb adsorption proceeds, the microbial activity of algal-bacterial AGS indicated by SOUR declined from 52.9 mg-O_2/g-MLSS·h to 8.5 mg-O_2/g-MLSS·h after 24 h. The integrity coefficient of algal-bacterial AGS with Pb also increased from 2.3% to 4.1%, indicating the decreased structure stability of granules. Possible reasons are as follows: (1) the lack of nutrients supply caused the decreased bioactivity of granules; (2) Pb, as a toxic metal, has the intrinsic characteristic that adversely affects microbial activity. Pb can be also captured by proteins and other biopolymers, which may result in inhibition and decreased viability of granules.

To study the kinetics of Pb(II) adsorption onto algal-bacterial AGS, the pseudo-first-order and pseudo-second-order models were used to fit the experimental data as presented in Figure 2-7. The experimental data better fitted to the pseudo-second-order model with a higher R^2 of 0.9645 (Inset of Figure 2-7) and an estimated adsorption capacity (q_e) of 13.29 mg/g, indicating that chemisorption rather than physical sorption was the rate-limiting step in Pb(II) biosorption onto algal-bacterial AGS (Li et al., 2019). It should be noted that a much longer contact time of 24 h was necessary for the algal-bacterial AGS to reach the adsorption equilibrium when compared to the equilibrium contact time of 1 h for the inactivated AGS and 6 h for the chemically modified dry AGS, suggesting that the microbial effect might be involved in Pb(II) biosorption onto the algal-bacterial AGS (Mohapatra et al., 2019; Shi et al., 2015). In the Pb-loaded algal-bacterial AGS, 65.8% of the adsorbed Pb was found in the intracellular part, while 34.2% was detected in the extracellular part. This observation revealed that the bioaccumulation of Pb into the microbial cells largely contributed to Pb removal by the algal-bacterial AGS. This finding is consistent with a previous study (Yang et al., 2020) reflecting the important role of microbial viability of algal-bacterial AGS in heavy metal biosorption. Since the Pb(II) concentration was almost unchanged after 24 h (Figure 2-5), the optimal contact time was determined as 24 h for the following experiments.

2.4.3. Biosorption isotherms

The initial concentration of adsorbate is one of the significant factors that provide the driving force and overcome the resistance between solid and liquid phases, thus affecting the adsorption performance (Liu et al., 2019a). The biosorption isotherms of algal-bacterial AGS were investigated using solutions with different initial Pb(II) concentrations ($C_{Pb(II)}$, 10-300

mg/L) and the results are shown in Figure 2-8. The Pb(II) adsorption capacity of algal-bacterial AGS gradually increased from 3.64 mg/g at the initial Pb(II) concentration of 10 mg/L to 45.33 mg/g at the initial Pb(II) concentration of 300 mg/L, while the corresponding removal efficiency (Figure 2-9) decreased from 65.6 ± 0.7% to 15.6 ± 0.9%. The increase of Pb(II) concentration in the solution can overcome the mass transfer resistances between the aqueous and solid phases, thus resulting in increased Pb adsorption capacity of algal-bacterial AGS at a higher initial Pb(II) concentration (Wang et al., 2022a). Langmuir and Freundlich isotherm models are two classic models to predict the absorbability of biosorbents. Thus, the experimental data were fitted to these two models (Inset of Figure 2-8), indicating that complex mechanisms may be involved in the Pb biosorption using algal-bacterial AGS. According to the Langmuir model, the theoretical maximum adsorption capacity was estimated as 72.4 mg/g, which is superior to most similar biosorbents (Table 2-3). Considering the quick cultivation, easy harvesting or separation, and excellent adsorption performance, the algal-bacterial AGS without pretreatment is proposed as a promising alternative to removing Pb(II) from wastewater.

2.4.4. Effect of coexisting ions

Generally, Pb(II) containing wastewater may also contain other HMs cations. Therefore, the effect of other co-existing ion (Cr, Cu, Zn, Cd) with different concentrations (5, 10, 20, 50 and 100 mg/L) on Pb(II) adsorption by algal-bacterial AGS as shown in Figure 2-10. It can be seen the presence of these cations has slight influence on Pb(II) removal by algal-bacterial AGS, which may confirm that they compete for he active sites with Pb(II) onto the granules. Generally, competitive adsorption ability varies from one metal to the other for the molecular mass, ion charges, hydrated ionic radius and hydration energy of the metals (Nassar, 2010). In this study, they compete with Pb(II), which indicate that the Pb(II) adsorption onto the granules is monolayer adsorption. This is consistent with the results of the adsorption isotherm.

2.4.5. Effect of granular dosage

Figure 2-11 shows the effect of granular dosage (0.2-10 g/L-MLSS) on the Pb(II) removal by algal-bacterial AGS. It can be seen that with the increase of granular dosage from 0.2 g/L to 10 g/L, the Pb(II) concentration in solution decrease from 45.26 ± 2.3 mg/L at 0.2 g/L to 0.06 ± 0.02 mg/L at 10 g/L. The corresponding adsorption capacity of algal-bacterial AGS decreases from 23.7 ± 0.68 mg/g to 4.94 ± 0.86 mg/g and the Pb(II) removal percentage increases from 9.48 ± 2.3% to 98.8 ± 0.02%. When the granule dosage is 1 g/L, the granule has a relatively better adsorption capacity of 12.35 ± 0.52 mg/g which is recommended for Pb(II)-containing wastewater treatment. When the granule dosage is 10 g/L, the Pb(II) concentration is 0.06 ± 0.02 mg/L which meets the emission standard of 0.1 mg/L.

2.5. Summary

In Chapter 2, the adsorption performance of algal-bacterial AGS on the Pb(II) removal was investigated with 5 typical parameters including pH, contact time and initial Pb(II) concentration, co-existing ion and granule dosage. The main results are as below:

1) Initial pH of 6.0 was determined as the optimal pH condition for Pb(II) biosorption by algal-bacterial AGS.
2) The reaction equilibrium was achieved at about 24 h with the biosorption process better fitted the pseudo-second-order kinetic model.
3) The biosorption isotherm better fitted the Langmuir isotherm model with a maximum adsorption capacity of 72.4 mg/g.
4) Co-existing ions (Cr, Cu, Zn, Cd) showed a slight influence on Pb(II) removal by algal-bacterial AGS.
5) When the granule dosage is 10 g/L, the Pb(II) concentration is 0.06 ± 0.02 mg/L which meets the effluent discharge standard.
6) Considering the quick cultivation, easy harvesting or separation, and excellent adsorption performance, the algal-bacterial AGS without pretreatment is proposed as a promising alternative to removing Pb(II) from wastewater.

Table 2-1 The composition of synthetic domestic wastewater used for the cultivation of algal-bacterial AGS.

Parameters	Concentration (mg/L, in the liquor)	Chemicals (mg/L, in the liquor))
COD	300	CH_3COONa (384)
NH_4^+-N	50	NH_4Cl (189)
Mg^{2+}	5	$MgSO_4 \cdot 7H_2O$ (51)
Fe^{2+}	5	$FeSO_4 \cdot 7H_2O$ (25)
Ca^{2+}	10	$CaCl_2 \cdot 2H_2O$ (41)
PO_4^{3-}-P	5	KH_2PO_4 (219)
Na^+	250	$NaHCO_3$(804)
Trace metals	1 mL/L	H_3BO_3 (50), $ZnCl_2$ (50), $CuCl_2$ (30), $MnSO_4 \cdot H_2O$ (50), $(NH_4)_6Mo_7O_{24} \cdot 4H_2O$ (50), $AlCl_3$ (50), $CoCl_2 \cdot 6H_2O$ (50), and $NiCl_2$ (50)

COD, chemical oxygen demand.

Table 2-2 The main characteristics and the average contents of main metal ions of algal-bacterial AGS after 14 days' cultivation.

Parameters	Algal-bacterial AGS
MLVSS (g/L)	4.31 ± 0.21
MLSS (g/L)	5.98 ± 0.11
MLVSS/MLSS (%)	72.1 ± 1.9
SVI_5 (mL/g-MLSS)	56.5 ± 2.3
Integrity coefficient (%)	5.5 ± 0.3
Chl-*a* (mg/g-MLSS)	5.3 ± 0.2
Metal ions (mg/g-MLSS)	
Na	8.18
K	9.20
Ca	10.76
Mg	7.12

Algal-bacterial AGS, algal-bacterial aerobic granular sludge; ML(V)SS, mixed liquor (volatile) suspended solids; SVI_5, sludge volume index at 5 minutes; Chl-*a*, Chlorophyll *a*. The data are shown as average ± standard deviation (n = 3).

Table 2-3 Comparison of Pb(II) biosorption performance using different biosorbents.

Biosorbents	pH	Dosage (g/L)	*T* (℃)	*t* (h)	$C_{Pb(II)}$ (mg/L)	q_m (mg/g)	Ref.
Brewer's yeast	5.0	4.5	30	24	55	1.8	(Ferraz and Teixeira, 1999)
Andean Sacha inchi	3.0	2.0	50	0.75	100	17.1	(Kumar et al., 2016)
Malva sylvestris flower	4.5	4.0	55	0.25	60	25.6	(Salahandish et al., 2016)
Cowpea pod	6.0	3.0	40	1	30	32.6	(Guyo and Moyo, 2017)
Capsicum annuum L. seeds	5.5	2.0	25	40 min	100	36.4	(Hammo et al., 2021)
Cassava peels	5.0	4.0	25	40 min	50	42.5	(Schwantes et al., 2016)
Fe_2O_3@Microalgal	5.3	0.5	25	1.5	80	62.6	(Shen et al., 2020)
Nitrified AGS	4.0	1.0	25	2.0	20	89.3	(Xu et al., 2020a)
Algal-bacterial AGS	6.0	1.0	25	24	50	72.4	This study

Note: *T*, reaction temperature, ℃; *t*, contact time, h; $C_{Pb(II)}$, initial Pb(II) concentration, mg/L; q_m, the maximum adsorption capacity, mg/g.

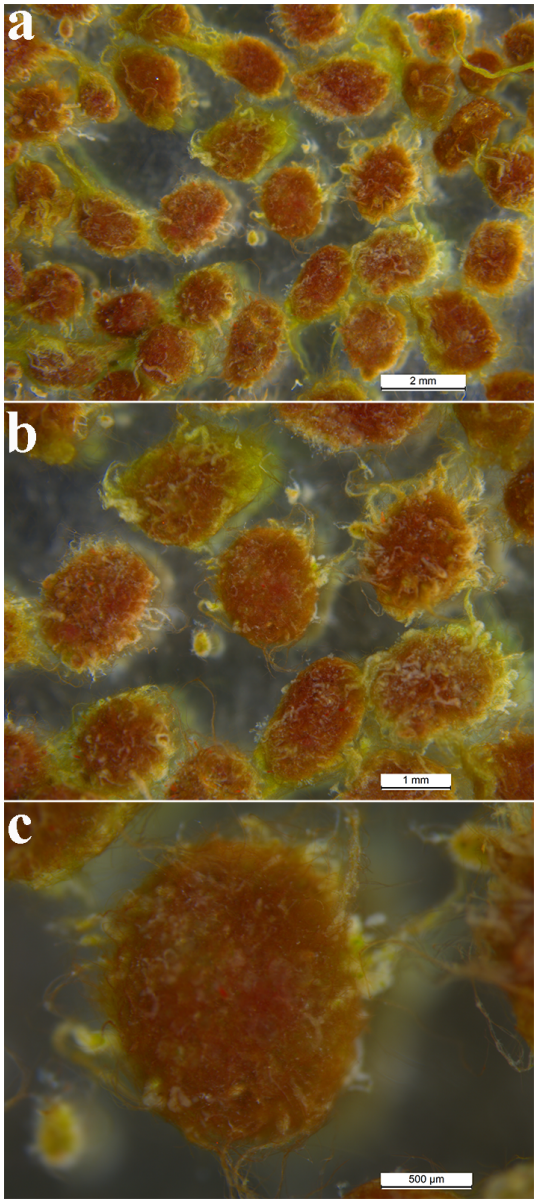

Figure 2-1. The microscopic images (a, b and c) of algal-bacterial AGS obtained after 14 days' cultivation.

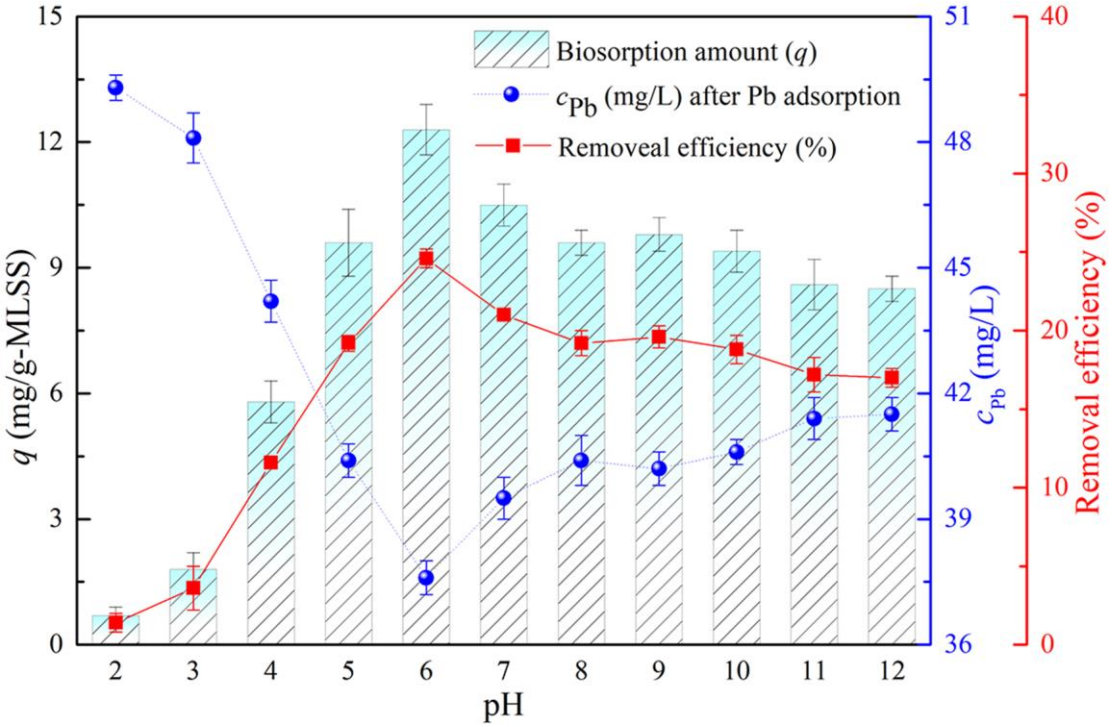

Figure 2-2. The effect of initial pH (2.0-12.0) on Pb(II) biosorption capacity and removal efficiency using algal-bacterial AGS (Initial Pb(II) concentration of 0-300 mg/L, contact time of 24 h). The data are shown as average ± standard deviation (n = 3).

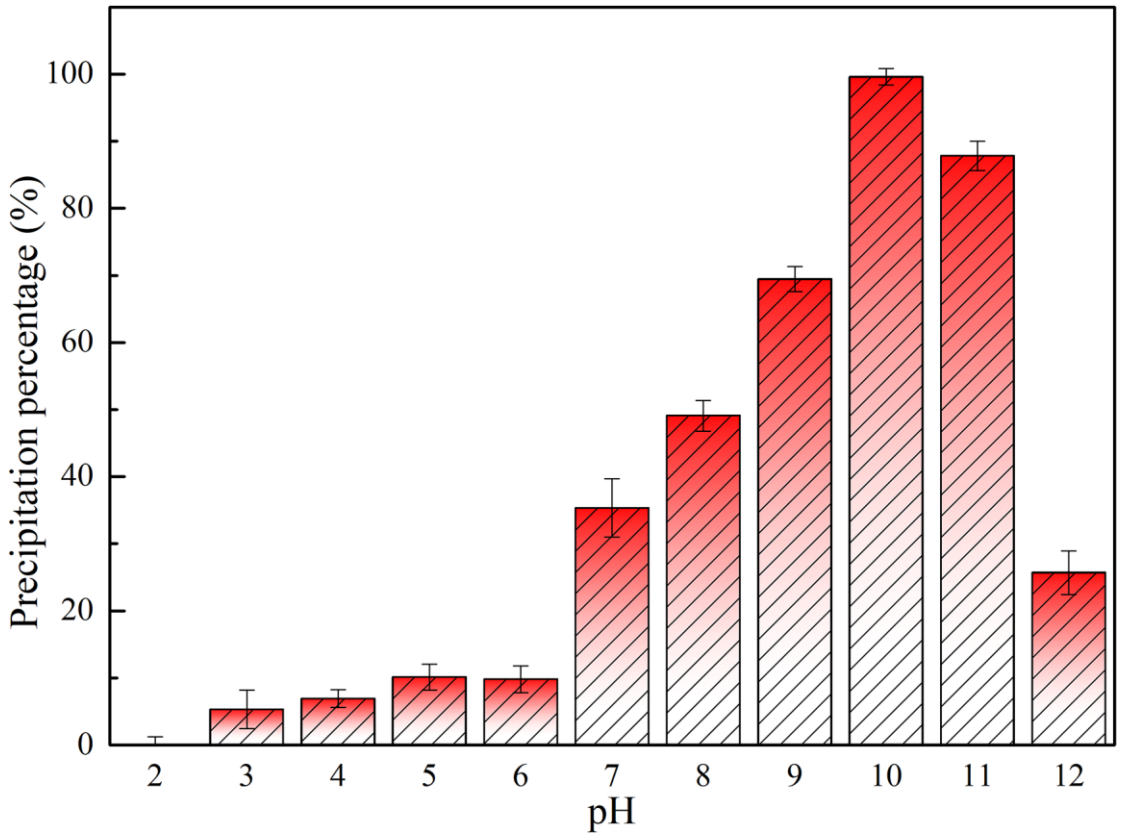

Figure 2-3. The precipitation percentage of the Pb at different pH (2.0-12.0). Initial Pb(II) concentration of 50 mg/L. The data are shown as average ± standard deviation (*n* = 3).

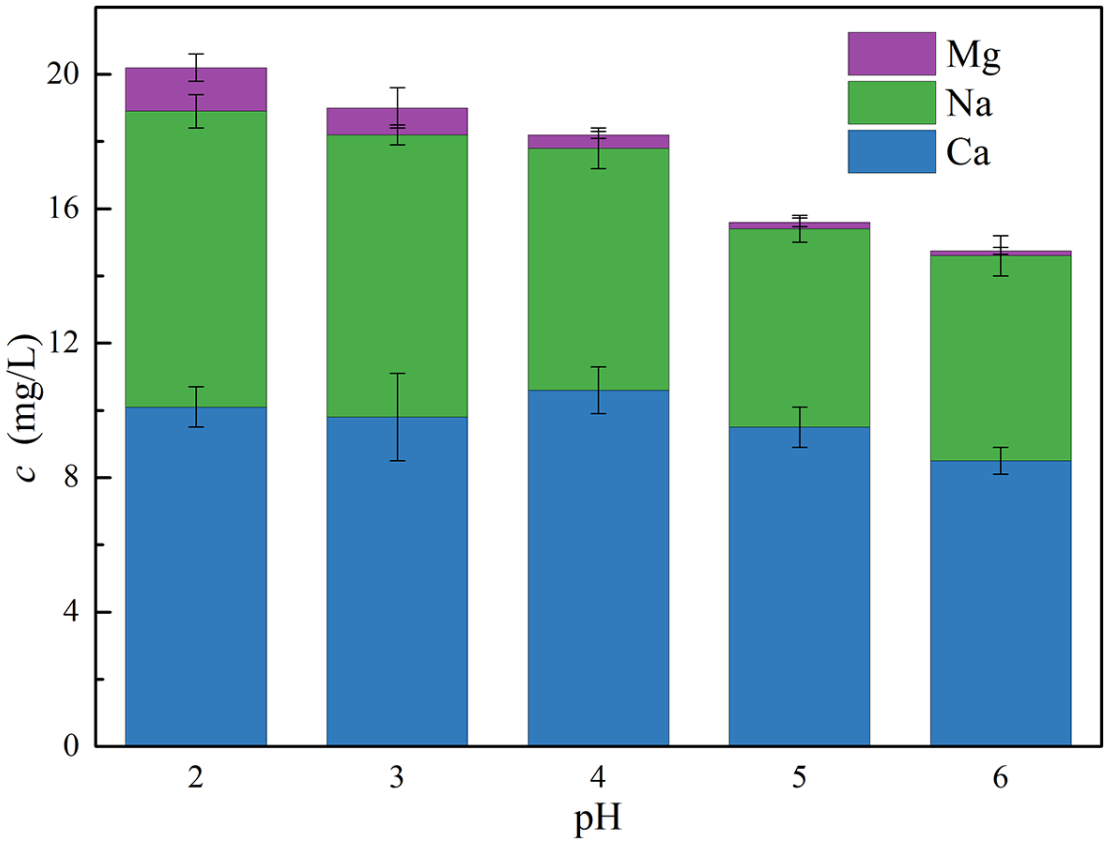

Figure 2-4. The concentrations of the released metal (Na, Mg, and Ca) ions in solutions after Pb(II) biosorption using algal-bacterial AGS at different initial pH (Initial pH 6.0, initial Pb(II) concentration of 50.0 mg/L and granule dosage of 1 g-MLSS/L). The data are shown as average ± standard deviation (n = 3).

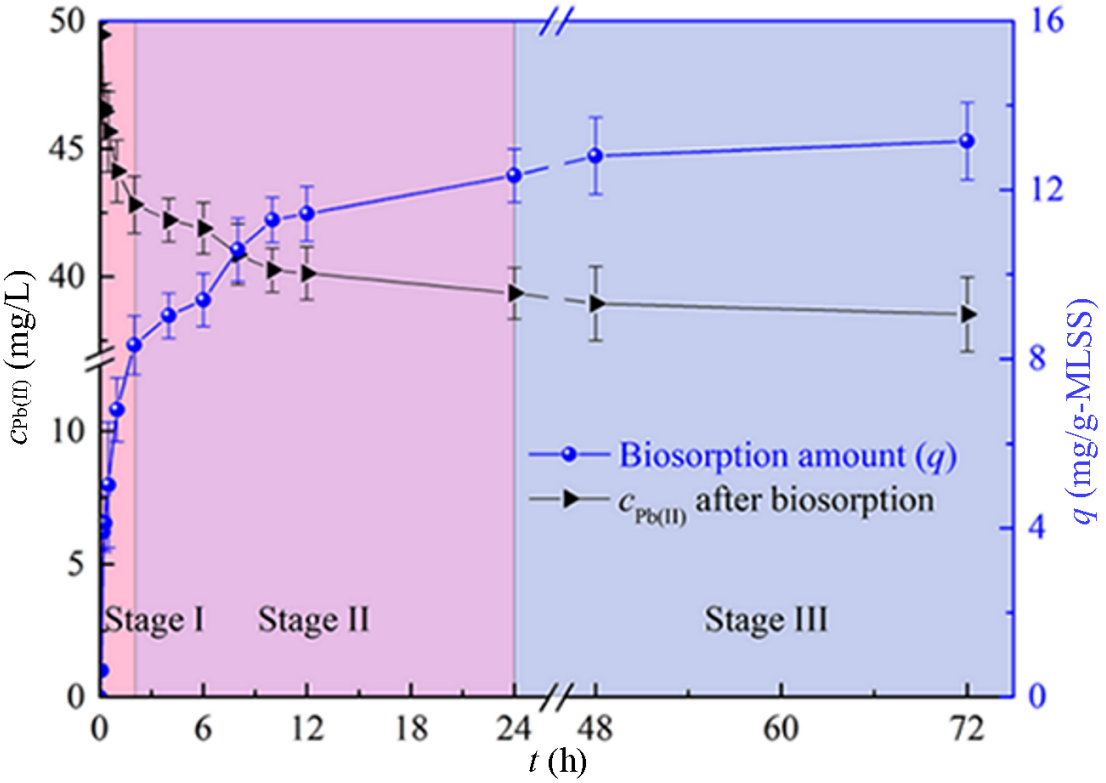

Figure 2-5. The effect of contact time (0-72 h) on the Pb(II) biosorption capacity using algal-bacterial AGS (Initial pH 6.0, initial Pb(II) concentration of 50.0 mg/L and granule dosage of 1 g-MLSS/L). The data are shown as average ± standard deviation (n = 3).

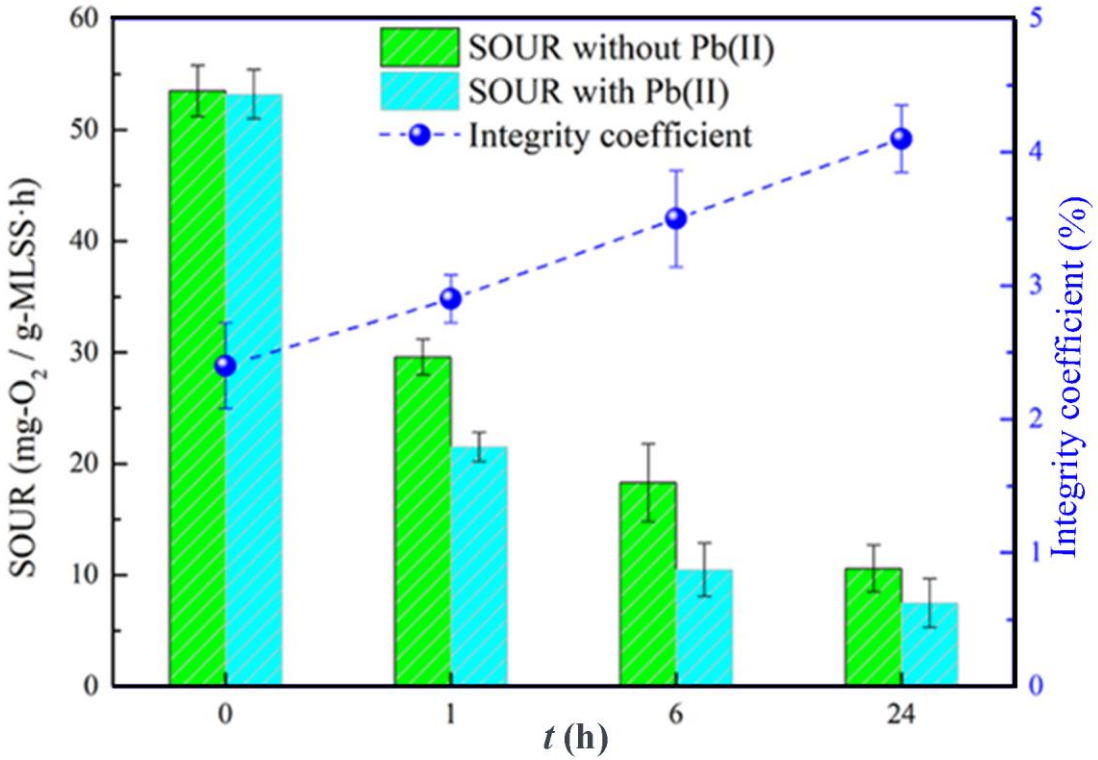

Figure 2-6. Variations of SOUR and integrity coefficient of algal-bacterial AGS at 0, 1, 6 and 24 h in the biosorption process with/without Pb(II) (Initial pH 6.0, initial Pb(II) concentration of 50.0 mg/L and granule dosage of 1 g-MLSS/L). The data are shown as average ± standard deviation (n = 3).

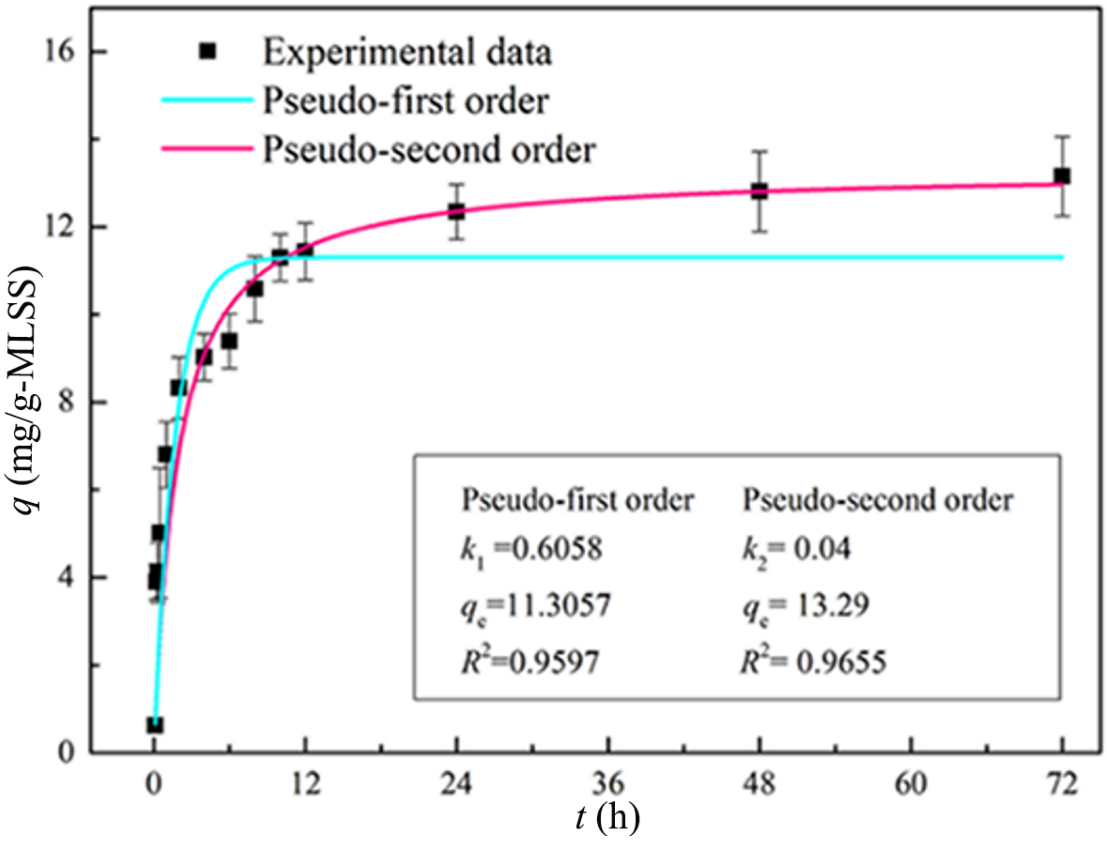

Figure 2-7. Adsorption kinetics analyzed by the pseudo-first-order model and pseudo-second-order model (Initial Pb(II) concentration of 0-300 mg/L, initial pH 6.). R^2 is the correlation coefficient; k_1 (min^{-1}) and k_2 ($g \cdot mg^{-1} \cdot min^{-1}$) are the rate constants of the pseudo-first-order and pseudo-second-order kinetic models, respectively; q_e (mg/g) is the equilibrium adsorption capacity calculated from kinetic models. The data are shown as average ± standard deviation (n = 3).

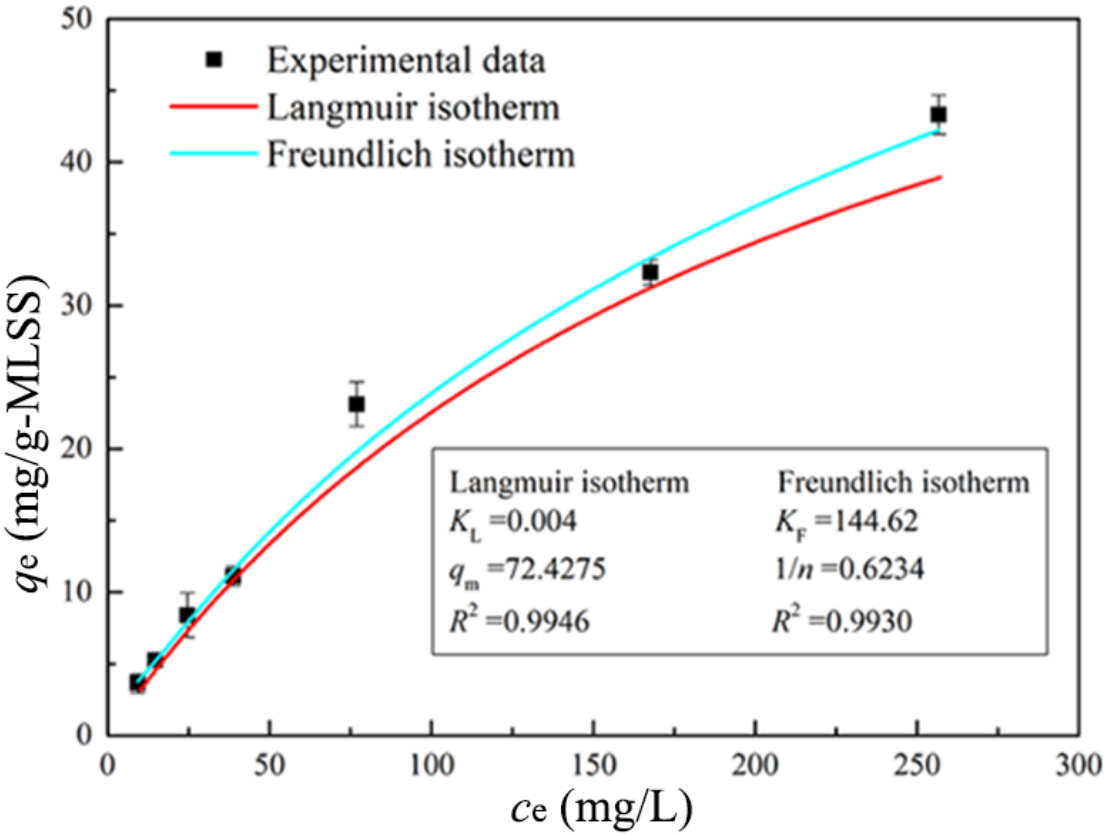

Figure 2-8. Adsorption isotherms analyzed by Langmuir and Freundlich isotherm models (Initial Pb(II) concentration of 0-300 mg/L, initial pH 6.0, contact time of 24 h). R^2 is the correlation coefficient; q_e (mg/g) is the equilibrium adsorption capacity calculated from kinetic models; q_m (mg/g) is the maximum adsorption capacity calculated from Langmuir isotherm model; K_L (L/mg^{-1}) and K_F (mg/g·(L/mg)$^{-1/n}$) are the Langmuir and Freundlich constants, respectively; 1/n is a dimensionless parameter. The data are shown as average ± standard deviation (n = 3).

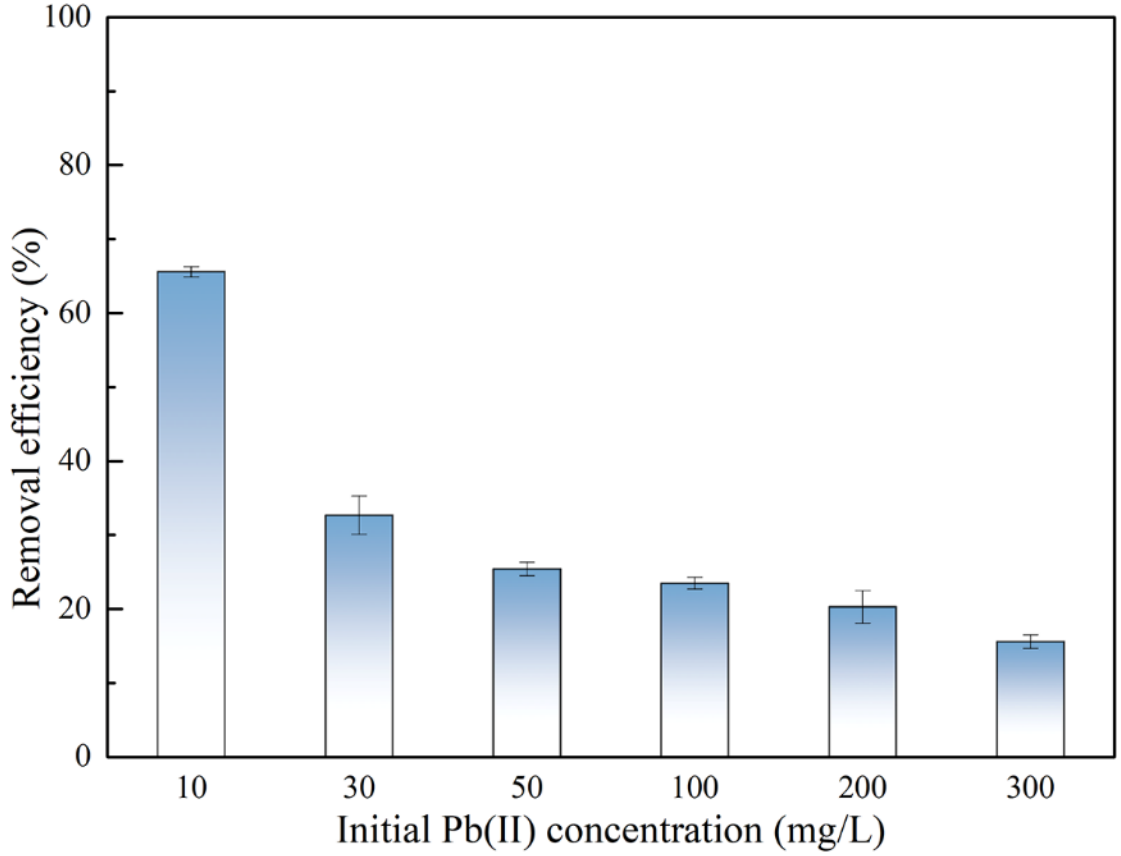

Figure 2-9. The removal efficiency of Pb(II) by algal-bacterial AGS at different initial Pb(II) concentrations (10-300 mg/L) (Initial pH of 6.0, granule dosage of 1 g-MLSS/L, contact time of 24 h). The data are shown as average ± standard deviation (n = 3).

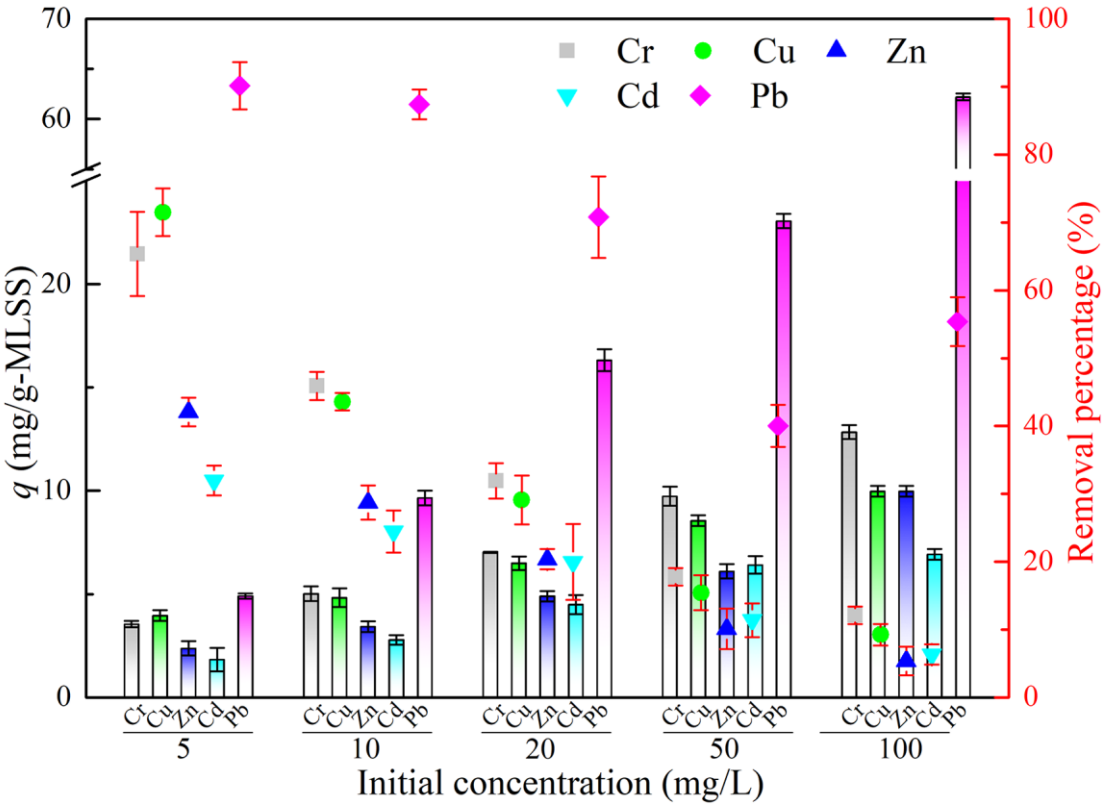

Figure 2-10. Effect of co-existing ion (Cr, Cu, Zn, Cd) with different concentrations (5, 10, 20, 50 and 100 mg/L) on biosorption capacity (*q*) and removal percentage of Pb(II) and the co-existing ion by algal-bacterial AGS (Initial pH of 6.0, granule dosage of 1 g-MLSS/L, contact time of 24 h). The data are shown as average ± standard deviation (*n* = 3).

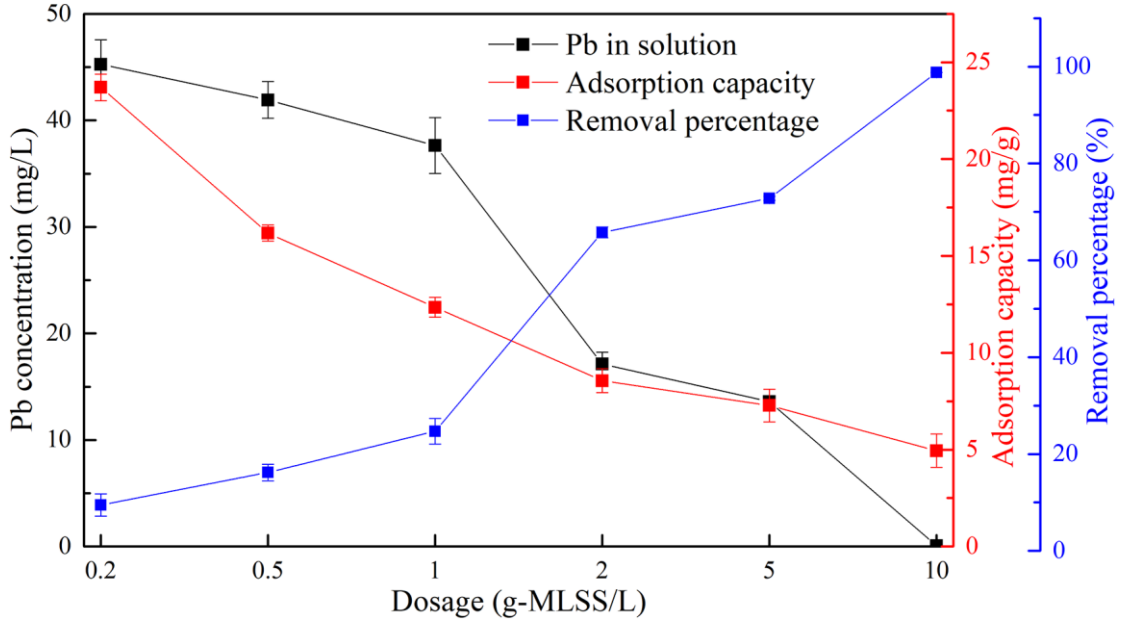

Figure 2-11. Effect of granular dosage (0.2-10 g-MLSS/L) on Pb(II) adsorption by algal-bacterial AGS (Initial pH of 6.0, initial Pb(II) concentration of 50.0 mg/L, granule dosage of 1 g-MLSS/L, contact time of 24 h). The data are shown as average ± standard deviation (n = 3).

Chapter 3 Biosorption mechanism of Pb(II) containing wastewater by algal-bacterial aerobic granular sludge

3.1. Introduction

In Chapter 2, the adsorption performance of algal-bacterial AGS for Pb(II) removal was investigated. At the same time, for granular sludge, extracellular polymeric substance (EPS) is one of the most important parts that can affect its physicochemical properties, microbial activity and adsorptive capacity (Cai et al., 2021). When granules were exposed to heavy metals, EPS will be excreted to resist interference, reduce the toxicity of heavy metals and maintain granular stability (Li et al., 2017a; Wei et al., 2016). Proteins (PN) and polysaccharides (PS), as two of the most important components of EPS, contain abundant metal ions (Ca, Mg, Fe, Na, etc.) and functional groups (hydroxyl group, carboxyl group, phosphate group and others), which can provide lots of active sites for heavy metal ions to ion exchange or bond. Electrostatic interaction, ion exchange, complexation and biomineralization usually take place between the HMs and EPS (Wang et al., 2014). Though extractive EPS could be used for HMs removal, (algal-bacterial) AGS may be a better choice considering a long-time and reusable operation. However, up to now, few studies are now available to comprehensively interpret the HMs removal like Pb(II) using algal-bacterial AGS, let alone the role of EPS in algal-bacterial AGS and the involved mechanism.

In this context, the objective of this study was to clarify the adsorption mechanism of Pb(II) removal, especially the role of EPS in the process.

3.2. Materials and methods

3.2.1. Characterization of algal-bacterial AGS

The MLSS, MLVSS and SVI_5 of the obtained algal-bacterial AGS were determined according to the standard methods. The Chl-*a* in algal-bacterial AGS was analyzed according to a previous study (Liu et al., 2019a). The morphology and size of algal-bacterial AGS were observed and measured using a Leica microscope (Leica M205C model).

3.2.2. Extracellular polymeric substances (EPS) extraction

For EPS extraction, a typical heating method was used (Wang et al., 2022b). Briefly, granules with or without Pb(II) after adsorption at pH of 6.0 and 25±1 ℃ were ground and added with 0.9% NaCl solution. The mixture was centrifuged at 7,500 g for 20 min with the supernatant after filtration was measured as the loosely bound EPS (LB-EPS). Then, another 0.9% NaCl solution was added to the residue and well mixed. After being heated at 80 °C for

30 min and centrifuged at 8,500 g for 20 min, the filtrated supernatant was analyzed as the tightly bound EPS (TB-EPS). For the analysis of proteins (PN) and polysaccharides (PS), the Lowry-Folin method and the phenol-sulfuric acid method were employed with bovine serum albumin (BSA) and glucose as the standards, respectively (Wang et al., 2022b).

3.2.3. Metal ion distribution

To investigate the distribution of Pb and other important metal ions (Ca, Na and Mg) in EPS, inductively coupled plasma atomic emission spectroscopy (ICP-AES, ICPS-8100 model, Shimadzu Co. ltd., Kyoto, Japan) was employed. To investigate the extracellular and intracellular distribution of Pb in the algal-bacterial AGS, a modified method from previous studies was used (Yang et al., 2021b). Briefly, the Pb-loaded algal-bacterial AGS after being washed with deionized water twice to remove the Pb(II) on the surface of granules. Then, the extracellular Pb content of algal-bacterial AGS was extracted using a 10% HCl solution. After shaking at 300 rpm for 5 min, the mixture was centrifuged at 4,900 g for 10 min to obtain the supernatant. The Pb concentration in the supernatant represented the extracellular Pb content. The total Pb content in algal-bacterial AGS was determined after the crushed algal-bacterial AGS was digested with nitrohydrochloric acid (concentrated HNO_3:HCl=3:1(v/v)). The intracellular Pb content was calculated by subtracting the extracellular Pb content from the total Pb content.

3.2.4. Physicochemical analyses

The algal-bacterial AGS samples before and after Pb(II) biosorption were dried at 40 ºC for 72 h and ground into powder for analyses using Fourier transform infrared (FT-IR, JASCO 6800 model) spectroscopy and X-ray diffraction (XRD, BrukerAXS D8 ADVANCE model). The algal-bacterial AGS powder (about 1 mg) was evenly mixed with KBr (about 200 mg) in an agate mortar, then squeezed by the manual press for 1 min to obtain a uniform translucent sample for FT-IR analysis at a frequency range of 4,000-400 cm^{-1}. The crystalline phase of algal-bacterial AGS powder was analyzed by XRD with Cu-Kα radiation at 2θ degrees ranging from 10 to 100 degrees. The obtained XRD pattern was then analyzed using the PDF-2(2014) database of the International Centre for Diffraction Data (ICDD) employed in the MDI Jade 6.0 software package.

3.2.5. Data analysis

All the experiments were conducted in duplicate, and the samples were analyzed in triplicate with the results being expressed as means or mean ± standard deviation. The *t*-test was applied to evaluate the significant differences in the results. All figures in this study were plotted using Origin 2019. The calculation method for the desorption ratio can be calculated by

Eq. (4-1) (Huang et al., 2019):

$$\text{Desorption percentage (\%)} = \frac{\text{Released metal amount}}{\text{Initially sorbed metal amount}} \times 100 \qquad (4\text{-}1)$$

3.3. Results and discussion

3.3.1. Role of EPS

(1) Keeping microbial activity

EPS is one of the important parts of algal-bacterial AGS, which affects the physicochemical properties and microbial activities of granules to a great extent (Liu et al., 2010). Proteins (PN) and polysaccharides (PS) are vital compositions for maintaining the framework of granules and their contents determine the stability and microbial activity to some extent (Wang et al., 2014). Figure 3-1 shows the changes of PN and PS contents, and PN/PS ratio in the Pb(II) adsorption process using algal-bacterial AGS. The PN and PS contents in EPS of raw algal-bacterial AGS were 251.30 ± 3.1 mg/g-MLSS and 49.80 ± 3.52 mg/g-MLSS, respectively, with a total EPS content (Total EPS ≈ Total PN + Total PS) of 301.10 ± 4.35 mg/g-MLSS and a PN/PS ratio of 5.05. As the adsorption proceeded to 48 h, the EPS content continuously decreased at both conditions (with/without Pb in solutions). The PS content changed a little, while the PN content decreased significantly, resulting in a significant reduction of total EPS content to 314.44 ± 2.9 mg/g-MLSS (control group) and 212.85 ± 2.45 mg/g-MLSS (with Pb group), and a lower PN/PS ratio of 4.13 (control group) and 3.96 (with Pb group). The possible reason could be attributed to little nutriment in the solution only containing 50 mg/L Pb(II), which causes the self-consumption of secreted EPS by microorganisms in algal-bacterial AGS to maintain their bioactivity. The existence of Pb in the solution resulted in a much lower content of PN, which may be because that Pb could get into the granules and block the internal channel, thus reducing substances transfer efficiency (Xiong and Liu, 2013). On the other hand, the significantly decreased SOUR (Figure 2-5b) implied that granules might be exposed to Pb indicating the inactivation of microorganisms and destruction of EPS structure, probably resulting in a decrease of EPS secretion (Zhu et al., 2012; Wang et a., 2018). These results indicated that EPS plays an important role in keeping the microbial activity of granules.

(2) Bonding to Pb

To reveal the bonding role of EPS for Pb removal, the Pb distribution in granules was analyzed. As shown in Figure 3-2, most of the adsorbed Pb was located in the residue (microbial cells and mineral particles), followed by the LB-EPS and TB-EPS. In the first 24 h, Pb content (Figure 3-4) in the residue part increased significantly compared to 0 h ($p = 1.261 \times 10^{-8} < 0.05$),

while the distribution in the three parts changed a little. From 24 h to 48 h, the Pb content in the residue was almost unchanged while the Pb content in LB-EPS and TB-EPS increased simultaneously. The Pb absorbed in microbial cells and formed mineral particles may be saturated and EPS played the main role in Pb removal after 24 h. Aerobic granules consist of many coccoid bacteria with a clearly defined boundary with high porosity on a coarse surface (Pagliaccia et al., 2022). As shown in Figure 3-3, algal-bacterial AGS before Pb adsorption (Figure 3-3a) had a compact and porous structure. After being exposed to Pb (Figure 3-3b), the granules became cracked and less sharply defined with numerous white deposits observed on their surface. When the granules are contacted with Pb, they may secrete more EPS to resist the pernicious effects of Pb (Wei et al., 2016). Besides, due to the continued accumulation of the Pb toxicity to algal-bacterial AGS, it may exceed the stability threshold of granules, which causes the apoptosis of microorganisms resulting in decreased EPS secretion. EPS is mainly composed of PN and PS, which possesses abundant functional groups that can provide bonding site for Pb. Therefore, the white deposits may form by bonding combination and further validation will be discussed in Section 3.3.2.3. Therefore, EPS may play an important role in bonding to Pb.

(3) Governing ions ingress and egress

In addition to PN and PS in EPS, metal ions including Ca, Na and Mg are also important components distributed in EPS (Sheng et al., 2010). In the biological processes, Ca^{2+} and Mg^{2+} can be absorbed and utilized by microorganisms (Wang et al., 2022b). Simultaneously, the binding between divalent cations and EPS is regarded as an essential intermolecular interaction to maintain the microbial aggregate structure (Guo et al., 2022). Therefore, the distribution and concentration variation of ions in EPS should not be ignored in the Pb biosorption process. Thus, the distribution and contents of the main ions (Ca, Na and Mg) in LB-EPS, TB-EPS and residue were analyzed. As shown in Figure 3-2, the total contents of Ca, Na and Mg in algal-bacterial AGS decreased continually in both groups (with/without Pb). In the meanwhile, the Pb contents in different parts (LB-EPS, TB-EPS and residue) of granules increased continuously, which showed significant increases after 24 and 48 h in residue ($p_{24\,h} = 1.261 \times 10^{-8}$ and $p_{48\,h} = 1.382 \times 10^{-8} < 0.05$) (Figure 3-4). The metal contents of Ca, Na and Mg in solution with Pb(II) were significantly increased ($p_{Ca} = 9.993 \times 10^{-8}$, $p_{Na} = 0.00001$ and $p_{Na} = 0.00449 < 0.05$) (Table 3-1) compared to the control group (without Pb). These results indicated that Pb may replace these metal ions in the granules. In the control group (without Pb), the Ca content decreased in LB-EPS and unchanged in TB-EPS, while Mg is almost unchanged in both LB-EPS and TB-EPS. This result interpreted that Ca may be more important for maintaining granule structure and livingness (Chen et al., 2013; Guo et al., 2022). In the group with Pb, Ca in LB-EPS decreased continually, and its proportion decreased at first and then increased. The release of metal ions may be because of the lower ion intensity in the solutions. In solution with Pb addition, more

Ca was released from algal-bacterial AGS, probably due to the ion exchange with Pb. The Ca content in TB-EPS was less affected at the beginning, which caused the increase of Ca proportion at first. As biosorption proceeded, more Pb entered into the internal part of granules, causing the decrease of Ca and Mg contents in TB-EPS (Figure 3-4). The significantly higher amount of Na released from granules in the Pb solution was also possibly attributed to ion exchange with Pb. In summary, the variations of metal ions (Ca, Na and Mg) indicated that EPS plays an important role in ions exchange and contributes to Pb biosorption.

All the above results demonstrated that EPS plays an important role in keeping microbial activity, Pb bonding and ion exchange with Ca, Na and Mg in algal-bacterial AGS.

3.3.2. Mechanisms analysis

The involved mechanisms in the Pb adsorption process using algal-bacterial AGS were proposed in Figure 3-5 with the distribution and variation of main parameters being summarized.

(1) Electrostatic interaction and cation exchange

At the beginning of biosorption (0 h), the granular surface and internal are in a dynamic equilibrium (Figure 3-5). When the granule was added to the Pb(II) solution, the surface charge and electrostatic repulsion first take effect as revealed by the increased adsorption capacity at increased initial pH values (Figure 2-2). Then, the Pb ion was migrated into LB-EPS, TB-EPS and finally the internal part through ion exchange with metal ions such as Ca, Na and Mg. Besides, LB-EPS responds firstly because it is located outside the TB-EPS and significant variation of metal ions can be observed at the first 6 h (proportion of ions changed from 30.6% Na, 16.2% Ca and 14.9% Mg at initial to 35.2% Na, 16.5% Ca and 14.9% Mg at 6 h) (Figure 3-2). With the Pb(II) biosorption proceeding, more metal ions (Ca, Na and Mg) would be transferred from the internal to external for ion exchange with Pb and increase the metal ion contents in the TB-EPS and LB-EPS (Figure 3-2). Therefore, metal ions in LB-EPS and TB-EPS increased to varying degrees after 24-h adsorption. To sum up, electrostatic interaction and ion exchange were involved in the Pb biosorption process using algal-bacterial AGS.

(2) Bonding to functional groups

The EPS content decreased from 240.9 mg/g-MLSS initially to 231.0 mg/g-MLSS at 6 h and 220.7 mg/g-MLSS at 24 h (Figure 3-1). The EPS contained not only such anions as nitrate, phosphate and sulfur functional groups, and the decrease of EPS content may be because the structure of granules was destroyed with Pb biosorption proceeded and the EPS was released to provide active sites for Pb bonding (Chen et al., 2013). To confirm this hypothesis, FT-IR spectra of algal-bacterial AGS before and after Pb(II) biosorption were used to investigate the

contribution of functional groups of algal-bacterial AGS to Pb(II) biosorption (Figure 3-5 and Table 3-2). The peak at 1,654 cm^{-1} is ascribed to the stretching vibration of the C=O bond in the carboxyl group or N-H in the amide I, which is usually found in amino acids, lipids, proteins, and carbohydrates (Gu and Lan, 2021; Nicomel et al., 2020). The bands near 1,076 cm^{-1} and 1,240 cm^{-1} correspond to the P=O bond in the phosphate group, a functional group of nucleic acids, phospholipids, phosphoproteins, and phosphosaccharides, etc. (Gu and Lan, 2021). The peaks at 2,924 cm^{-1} and 2,960 cm^{-1} represent the stretching vibration of C–H, which can be found in dextran functional groups on the cell wall of algal (Gu and Lan, 2021). Other important peaks at 1,040 cm^{-1}, 1,448 cm^{-1} and 3,292 cm^{-1} are ascribed to C-O-C (anhydride), CH- (alkane, methyl group) and O-H (carboxylic acid), respectively (Nicomel et al., 2020). Some shift of stretching vibrations of peaks at around 1,396 cm^{-1} and 1,543 cm^{-1} before biosorption to 1,383 cm^{-1} and 1,539 cm^{-1} after adsorption was noticed, probably due to the binding of Pb(II) to -COOH and amide (N-H and C-N bond) in the algal-bacterial AGS (Nicomel et al., 2020). A slight shift of stretching vibration of the peak at 1,237.55 cm^{-1} before biosorption to 1,236.00 cm^{-1} after biosorption was observed, indicating that the P=O group participated in the Pb(II) biosorption process. Furthermore, they may form insoluble compounds like $Pb_5(PO_4)_3Cl$ (Meng et al., 2020; Xu et al., 2020b), $Pb_5(PO_4)_3OH$ (Zhao et al., 2020), $PbCO_3$ (Mal et al., 2021), and other organic lead compounds. Recent studies have also shown that algal-based biosorbents cultivated in high-phosphorus or high-dissolved inorganic carbon cultures possess a higher Pb(II) removal performance (Chen et al., 2018; Yetis et al., 2000). In this study, -COOH, C-H, amide (N-H and C-N bonds) and P=O bonds were found to be the main functional groups that are liable for Pb(II) biosorption onto algal-bacterial AGS. Interestingly, adsorbed Pb was mainly located in the residue parts of the granule (Figure 3-4) even though significant changes in metal ions (Figure 3-2) were observed. Therefore, the bonding to functional groups and bioaccumulation of Pb into microbial cells probably take an important role in Pb biosorption using algal-bacterial AGS.

(3) Precipitation formation

To further confirm the bioaccumulation and identify the changes in chemical composition, XRD was used to analyze algal-bacterial AGS before and after Pb(II) biosorption (Figure 3-6). The chemical composition of algal-bacterial AGS before Pb(II) biosorption was typically composed of polysaccharides and fatty acids (Klik et al., 2021; Yang et al., 2021b). After Pb(II) biosorption, some variations were observed at 20.6°, 21.5°, 27.4°, 30.1°, 31.0° and 43.8°, etc., which match the characteristic peaks of pyromorphite ($Pb_5(PO_4)_3Cl$, PDF#19-0701). Pyromorphite is well known as the most stable Pb mineral existing on the earth with very low solubility (Gu et al., 2021). Thus, the formation of Pb(II) precipitate could contribute to Pb(II) removal by algal-bacterial AGS, which also can be confirmed by numerous white deposits observed on the granules' surface after Pb adsorption (Figure 3-3). Considering the results of

FT-IR and XRD, bioaccumulation and formation of precipitate may simultaneously be involved in the Pb(II) biosorption on algal-bacterial AGS.

Based on all the above, Pb(II) biosorption on algal-bacterial AGS was contributed by both physicochemical and biological effects, and the possible mechanisms including electrostatic interaction, ion exchange, and bonding to functional groups might take effects in the Pb adsorption process using algal-bacterial AGS. Then, over 60% of the adsorbed Pb is located in the residue (microbial cells or mineral particles) through bioaccumulation and the formation of pyromorphite precipitate ($Pb_5(PO_4)_3Cl$).

3.4. Summary

In this chapter, Pb removal mechanisms were investigated with the role of EPS being analyzed. The main results are as below: EPS play an important role in keeping microbial activity, Pb bonding, and ion exchange in algal-bacterial AGS. Both physicochemical and biological effects were involved in biosorption. Electrostatic interaction, ion exchange, and bonding to functional groups orderly contributed to Pb(II) biosorption. Under the conditions of this experiment, 66% of the adsorbed Pb was located in the residue part (microbial cells or mineral particles) by bioaccumulation and the formation of pyromorphite precipitate ($Pb_5(PO_4)_3Cl$).

Table 3-1 The average contents of the released main metal ions (Na, Mg and Ca, mg/L) into the solution in the absence and presence of Pb(II) with the addition of algal-bacterial AGS.

	Na	*p*-value	Mg	*p*-value	Ca	*p*-value
Without Pb(II)	4.85±0.26	-	0.11±0.06	-	6.42±0.39	-
With Pb(II)	6.12±0.39***	0.0000143	0.23±0.1*	0.00449	8.05±0.4***	9.993×10^{-8}

Experimental conditions: initial pH of 6.0, initial Pb(II) concentration of 50.0 mg/L, granule dosage of 1 g/L, contact time of 24 h. The data are shown as average ± standard deviation (n = 3). Significant differences between without and with Pb(II) groups were shown as * $p < 0.05$, ** $p < 0.01$, *** $p < 0.001$. Differences between groups were analyzed using the *t*-test.

Table 3-2 FT-IR peaks of algal-bacterial AGS before and after Pb(II) adsorption (Xu et al., 2020b; Zhao et al., 2020).

Wavelength (cm^{-1})		Functional groups
Algal-bacterial AGS	Pb-loaded algal-bacterial AGS	
1042.66	1035.70	C-O-C
1078.24	1074.37	C-O-C
1237.55	1236.00	P=O
1396.09	1383.72	-COOH
1448.68	1447.91	-COOH
1543.03	1539.93	C-N
1653.62	1654.39	C=O
2928.89	2929.67	$-CH_n-$
2959.05	2959.59	$-CH_n-$
3291.60	3293.92	-OH

pH of 6.0, initial Pb(II) concentration of 50.0 mg/L, granule dosage of 1 g-MLSS/L, contact time of 24 h.

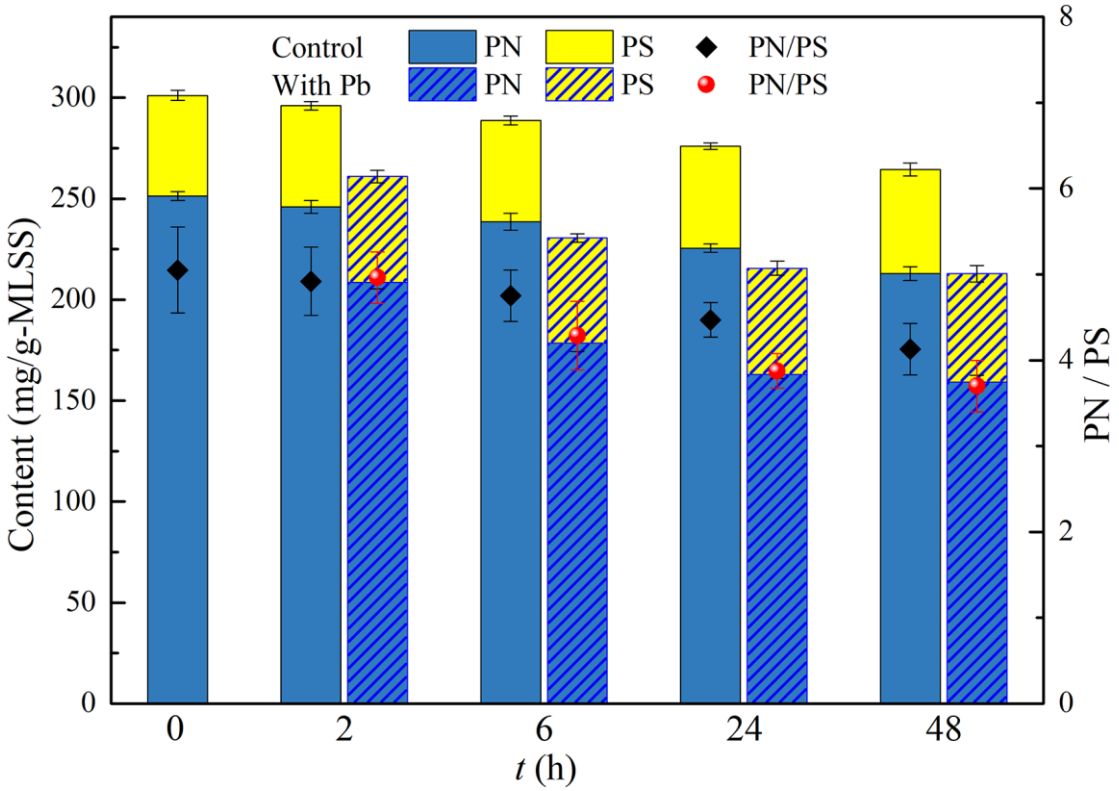

Figure 3-1. Variations of PN and PS contents, and PN/PS ratio in EPS of algal-bacterial AGS at different contact time. Biosorption conditions: initial pH of 6.0, granule dosage of 1 g-MLSS/L, and initial Pb concentration of 0 (control) or 50 mg/L (With Pb). PN, proteins; PS, polysaccharide. The data are shown as average ± standard deviation (n = 3).

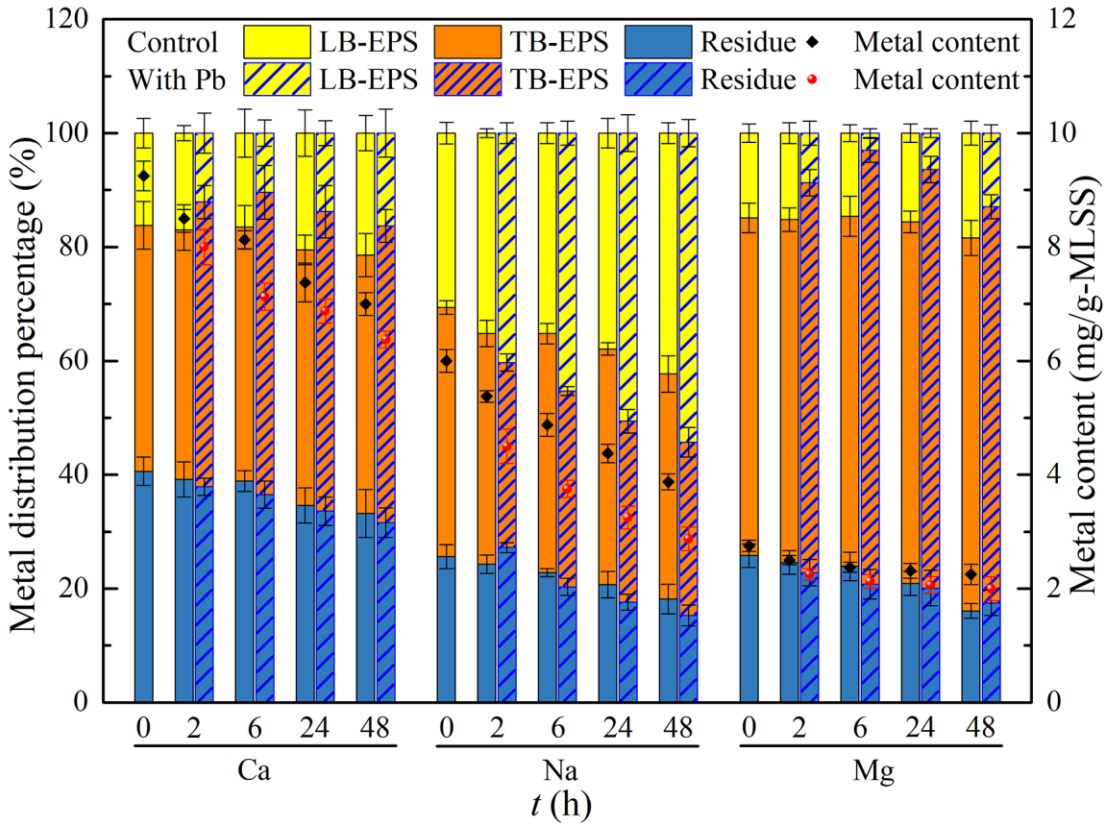

Figure 3-2. Variations of distribution and contents of metals (Ca, Na, Mg) in EPS of algal-bacterial AGS at different contact time. Biosorption conditions: initial pH of 6.0, granule dosage of 1 g-MLSS/L, and initial Pb concentration of 0 (control) or 50 mg/L (With Pb). LB-EPS, loosely bound EPS; TB-EPS, tightly bound EPS; Residue, microbial cells and mineral particles. The data are shown as average ± standard deviation (n = 3).

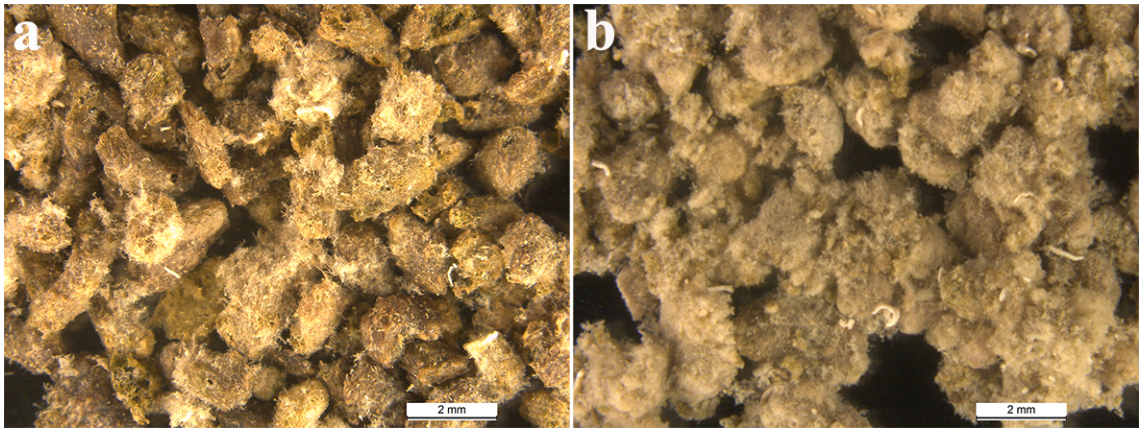

Figure 3-3. The optical photographs of algal-bacterial AGS (a) before and (b) after Pb adsorption treated by lyophilization. Experimental conditions: Initial pH of 6.0, initial Pb(II) concentration of 50.0 mg/L, granular dosage of 1 g-MLSS/L, contact time of 24 h.

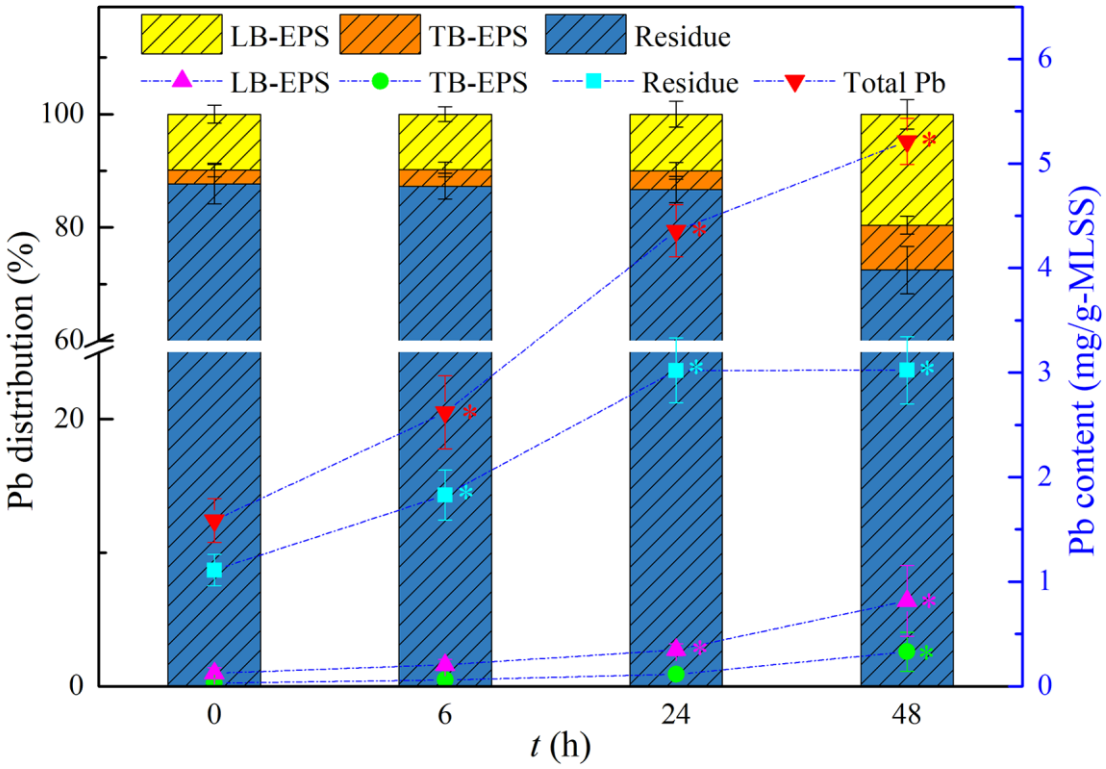

Figure 3-4. Variations of distribution and contents of Pb in EPS and residue part of algal-bacterial AGS at different contact time. Biosorption conditions: initial pH of 6.0, granule dosage of 1 g-MLSS/L, and initial Pb concentration of 0 (control) or 50 mg/L (With Pb). LB-EPS, loosely bound EPS; TB-EPS, tightly bound EPS; Residue, microbial cells and mineral particles. Significance analysis was performed to compare Pb content at different time in each part to that at 0 h using *t*-test. * $p < 0.05$.

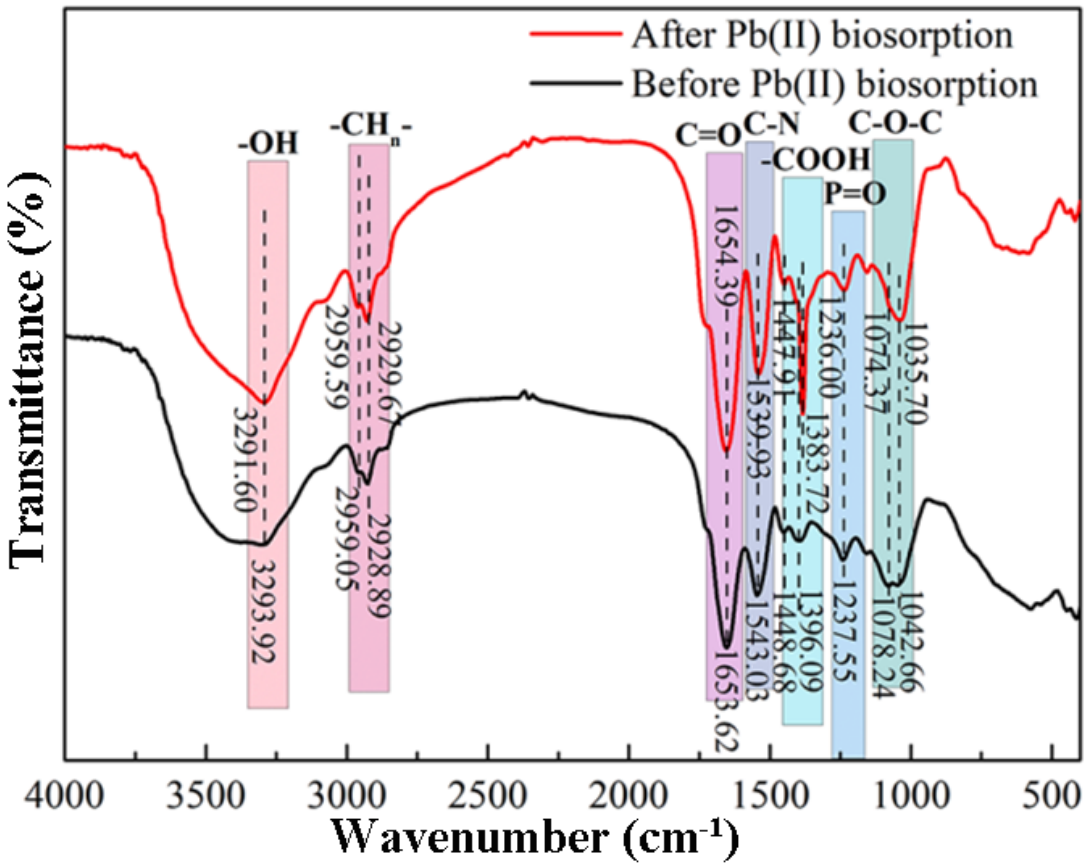

Figure 3-5. FT-IR spectra of algal-bacterial AGS before (black line) and after (red line) Pb(II) biosorption. The biosorption experiment was performed in 50 mg/L of Pb(II) solution with a granule dosage of 1 g-MLSS/L at an initial pH of 6.0 for contacting 24 h.

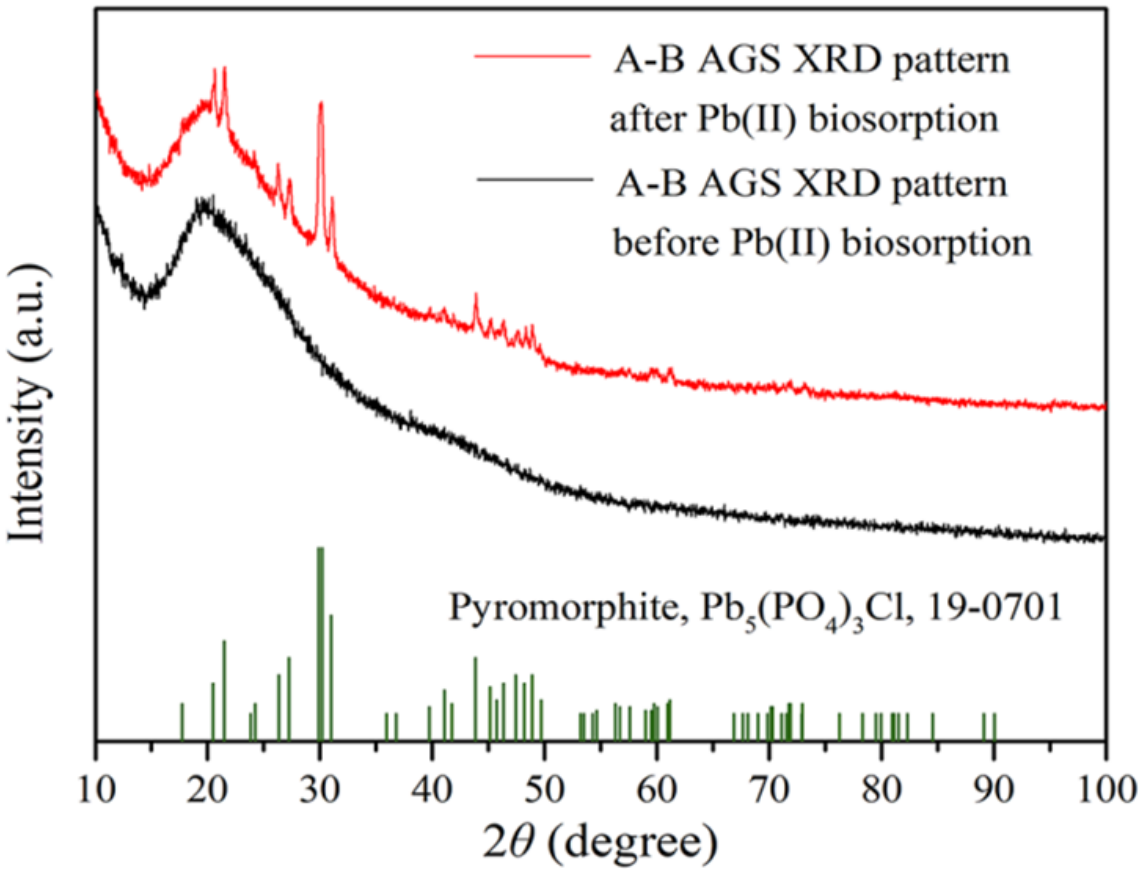

Figure 3-6. XRD pattern of algal-bacterial AGS before (black line) and after (red line) Pb(II) biosorption. The biosorption experiment was performed in 50 mg/L of Pb(II) solution with a granule dosage of 1 g-MLSS/L at an initial pH of 6.0 for contacting 24 h. A-B AGS, algal-bacterial AGS.

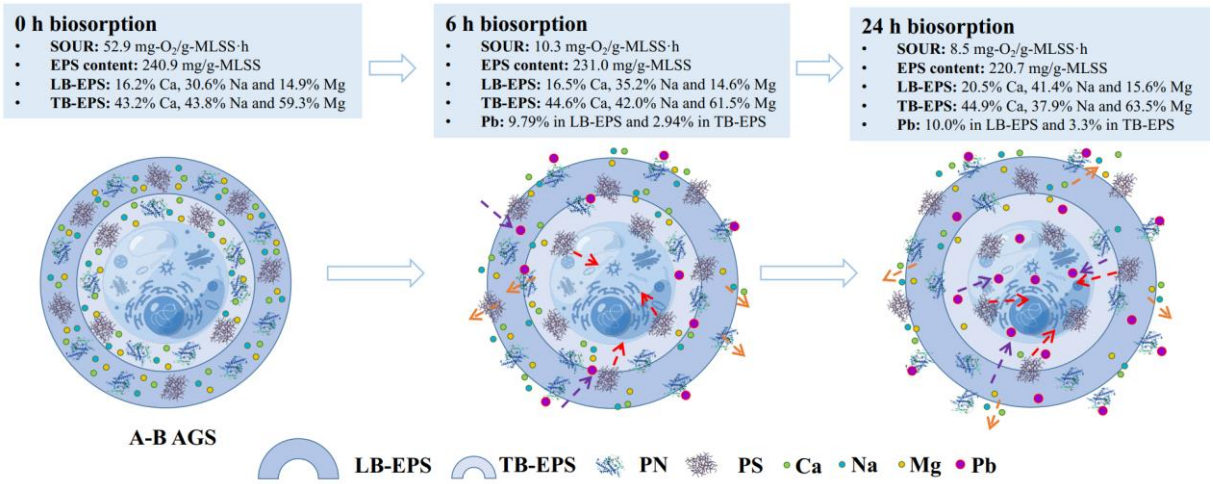

Figure 3-7. Variations of microbial activity (indicated by SOUR), EPS contents and metals distribution in the EPS of algal-bacterial AGS, and schematic diagram of the possible biosorption mechanisms in the Pb(II) biosorption process using algal-bacterial AGS.

Chapter 4 Pb(II) distribution and desorption from Pb-loaded algal-bacterial AGS

4.1. Introduction

In Chapters 2 and 3, the adsorption performance and the removal mechanism of the algal-bacterial AGS for Pb(II) were investigated and analyzed. However, the bioactivity of the granules became lower after Pb(II) adsorption. To recover adsorbed Pb from Pb-loaded algal-bacterial AGS and keep its bioactivity, proper methods should be adopted and the Pb(II) distribution in the granules should be revealed.

In this context, the objective of this chapter was to analyze the metal composition distribution in the Pb-loaded algal-bacterial AGS and explore optimal reagent to desorb Pb(II) from Pb-loaded granules.

4.2. Materials and methods

4.2.1. Cultivation of algal-bacterial AGS

The algal-bacterial AGS used in this study is the same with Section 2.2.1. In brief, the two SBRs were operated at room temperature (25±2 ℃) with a typical operation cycle of 6 h and an exchange ratio of 50%, resulting in a hydraulic retention time (HRT) of 12 h. Each cycle included 15-min feeding, 90-min non-aeration, 251-min aeration, 2-min settling, and 2-min effluent discharge. Artificial light with an illuminance of 3,000 lux was applied continuously (24 h/day) from the sidewall of the reactor to promote the formation of algal-bacterial AGS. After that, the granules were obtained and used for the subsequent experiments. The detailed characteristics of the cultivated algal-bacterial AGS are shown in Table 2-2.

4.2.2. Desorption experiments

The Pb-loaded algal-bacterial AGS were obtained after 24-h biosorption in 50 mg/L of Pb(II) solution with an algal-bacterial AGS dosage of 1 g/L at an initial pH of 6.0. The Pb-loaded algal-bacterial AGS were washed with deionized water three times until no Pb(II) was detected in the rinse solution. Several reagents including deionized water, acids (H_2SO_4, HCl and HNO_3), alkali (NaOH), salts (Na_2CO_3, $CaCl_2$, CH_3COONa) and chelating agents (EDTA and Na_2EDTA) with a concentration of 0.01 M-0.05 M were trialed for Pb(II) desorption. The desorption experiments were conducted in 20 mL of desorption reagent at a Pb-loaded algal-bacterial AGS dosage of 1 g/L. The mixture was shaken at 100 rpm and 25 ± 1 ºC for 6 h. Finally, the Pb(II) concentrations in the desorbents were determined after the crushed algal-bacterial AGS was digested with nitrohydrochloric acid (concentrated HNO_3:HCl=3:1(v/v)).

The intracellular Pb content was calculated by subtracting the extracellular Pb content from the total Pb content.

4.2.3. Pb distribution

To analyze the Pb composition, the chemical fractionations of metals in the Pb-loaded algal-bacterial AGS were analyzed according to the previous procedures (Tessier et al., 1979). The metals in the granules can be divided into 6 parts: (1) F1, Water soluble; (2) F2, exchange; (3) F3, carbonate bound; (4) F4, Fe/Mn oxides bounds; (5) F5, Organic bound; (6) F6, residue. The detailed methods are shown in Table 4-1.

4.2.4. Data analysis

All the experiments were conducted in duplicate, and the samples were analyzed in triplicate with the results being expressed as means or mean ± standard deviation (SD). All figures in this study were plotted using Origin 2019.

4.3 Results and discussion

4.3.1. Metal composition

To analyze the metal composition in the Pb-loaded algal-bacterial AGS, the metals distribution in the Pb-loaded algal-bacterial AGS in the case of chemical percentage (Figure 4-1) and intra/extracellular distribution (Figure 4-2) were analyzed. According to the previous report, the metal compositions were divided into 6 parts (F1, water soluble; F2, exchange; F3, carbonate bound; F4, Fe/Mn oxides bounds; F5, organic bound; F6, residue) including mobile parts (F1, F2 and F3) and stable parts (F4, F5 and F6). Mobile parts are available to biota or leached into the environment while the stable parts are relatively not bioavailable except the extreme situations. At the same time, the residue parts may not be able to be released under natural conditions at short time (Nair et al., 2008). As can be seen from Figure 4-1, for Pb, 61.3 ± 3.8% and 3.1 ± 1.2% of the adsorbed Pb are in the organic bound or residue fraction parts while the mobility factor (MF) value (MF=F1+F2+F3) was 22.6%. For Fe, the MF value (12.1%) is lower than the residue part (14.2%). At the same time, it is different in the case of MF value of light metals including Ca (84.3%) and Mg (78.5%). These were in agreement with previous reports that light metals are usually released from the biosorbents in the process of HMs removal (Wang et al., 2010; Xu and Liu, 2008). Besides, the trends of metal composition were in agreement with the results of intra/extracellular distribution (Figure 4-2). Over 60% of Pb was intracellularly immobilized but the proportion decreased to less than 45% for Mg or Ca, implying that the extracellular part of metals in algal-bacterial AGS were more likely to be mobile forms.

4.3.2. Pb desorption

A suitable desorbent is vital to the downstream separation and recycling process after biosorption (Bayuseno and Schmahl, 2011). Several types of reagents including acids, alkali, salts and chelating agents were tested for Pb(II) desorption from the Pb-loaded algal-bacterial AGS. As shown in Figure 4-3, all the desorbents showed relatively higher desorption performance (1.80-60.26%) than deionized water (DW, 1.02 ± 0.23%). The highest desorption ratio of 60.26 ± 3.23% was achieved by 0.05 M Na_2EDTA solution, followed by 0.05 M HCl (58.33 ± 1.65%) and 0.05 M EDTA (50.64 ± 2.23%). Besides, 0.05 M Na_2EDTA solution (Figure 4-4) was confirmed to be better than Pb(II) desorption considering the chemicals cost and desorption ratio. The higher efficiency of Na_2EDTA for Pb desorption is ascribed to the fact that EDTA has a stronger ligand with COOH groups (Yang et al., 2022). Besides, it is also possible that Na^+ and H^+ ions in Na_2EDTA solution may replace Pb to form the H_3O^+ and compete for the adsorption sites with stable water-soluble complexes of Pb that have weak adsorption ability to the granules (Yang et al., 2022). This observation also indicated that the chelating agents with excellent metal complex capacity and acidic pH may help to release and capture Pb(II) adsorbed on the algal-bacterial AGS. It should be noted that 0.05 M H_2SO_4 demonstrated a significantly lower desorption performance (1.80 ± 0.63%) than other acids while the use of 0.1 M H_2SO_4 achieved a Cr desorption ratio of 33.5 ± 2.6% from Cr-loaded algal-bacterial AGS (Yang et al., 2020). Although the acidic reagents may help to destruct the cell structure to release Pb(II) from algal-bacterial AGS, Pb(II) may form precipitates with SO_4^{2-}, probably resulting in channel clogging of granules and a lower Pb(II) concentration in the solution (Bayuseno and Schmahl, 2011). While this precipitation phenomenon would not happen in the case of Cr desorption due to its main existing form of $Cr_2O_7^{2-}$, in agreement with the higher Cr desorption ratio from Cr-loaded algal-bacterial AGS. On the other hand, the SOUR of algal-bacterial AGS, which represents the microbial activity of granules, was determined before and after Pb desorption. As seen in Figure 2-5, the highest SOUR of algal-bacterial AGS remained after desorption by 0.05 M Na_2EDTA, indicating its less impact on microbial activity and the possibility of recycling algal-bacterial AGS for wastewater treatment, which is still under investigation. Results showed that among the tested reagents, Na_2EDTA solution is the most efficient and safe desorbent to recover Pb(II) from the Pb-loaded algal-bacterial AGS.

4.4 Summary

In chapter 4, the Pb(II) distribution and the desorption by chemical desorption methods from Pb-loaded algal-bacterial AGS were studied. For the adsorbed Pb in algal-bacterial AGS, 61.3% and 3.1% of the adsorbed Pb were in the organic-bound or residue fractions while 22.6%

was found in the mobile fraction. 60.3% of the loaded Pb could be recovered using Na_2EDTA (0.05 mol/L). Over 60% of Pb was intracellularly immobilized but the proportion for Mg or Ca was 45%, implying that the metals located in the extracellular part of algal-bacterial AGS were more likely to be mobile forms.

All the findings from this study are expected to provide the theoretical basis for the large-scale application of algal-bacterial AGS for cost-effective biosorption of Pb(II)-containing wastewater, contributing to mitigating the Pb-derived environmental pollution and health risk.

Table 4-1 The extraction procedures for the metal ions (Tessier et al., 1979).

Fraction	Methods
F1, water soluble	The 0.1 g (dry weight) sample was used to extract with 4 mL of DW at room temperature (25 ± 2 °C) for 1 h under continuous shaking.
F2, exchangeable	The residue from F1 was extracted with 4 mL of 1 M NH_4OAc, at pH 7 and room temperature for 2 h under continuous shaking.
F3, carbonate bound	The residue from F2 was leached with 4 mL of 1 M NH_4OAc at pH 5 (adjusted with acetic acid) and room temperature (25 ± 2 °C) for 2 h under continuous shaking.
F4, Fe/Mn oxides bounds	The residue from F3 was extracted with 4 mL of 0.04 M hydroxylamine hydrochloride ($NH_2OH{\cdot}HCl$) in 25% acetic acid (v/v) at pH 3 and 80 °C for 6 h under occasional shaking.
F5, organic bound	The residue from F4 was extracted with 3 mL 30% H_2O_2 (with pH being adjusted to 2 with HNO_3) at 80 °C for 5.5 h under occasional shaking. After cooling down, 1 mL of 3.2 M NH_4OAc in 20% (v/v) HNO_3 was added with the sample volume being adjusted to 4 mL using DW, and then the sample was continuously shaken at room temperature (25 ± 2 °C) for 0.5 h.
F6, residue	The residue from F5 was digested with HNO_3 and H_2SO_4 at 120 °C for 12 h under occasional shaking.

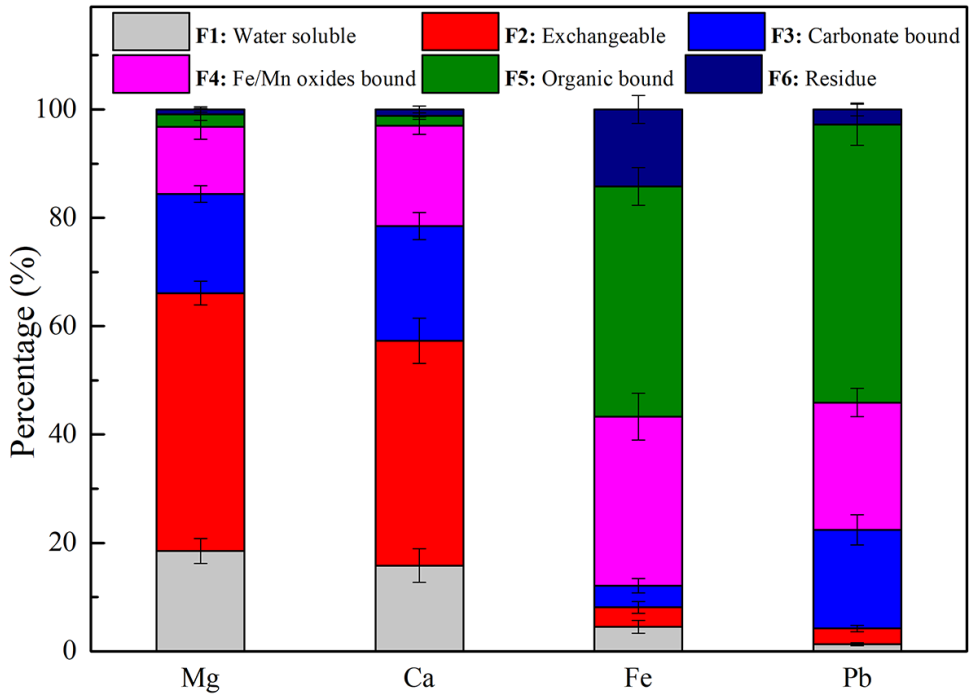

Figure 4-1. The chemical percentage of metals in the Pb-loaded algal-bacterial AGS. The data are shown as average ± standard deviation (n = 3).

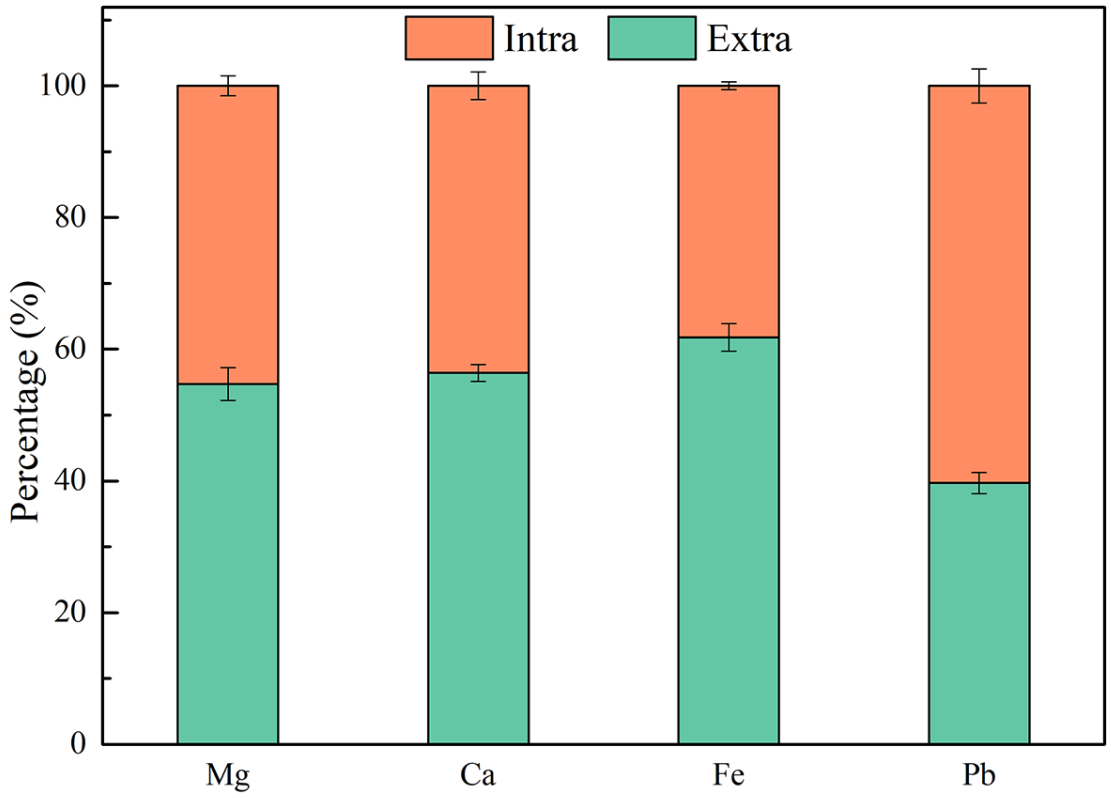

Figure 4-2. The metal intra/extracellular distribution in the Pb-loaded algal-bacterial AGS. The data are shown as average ± standard deviation (n = 3).

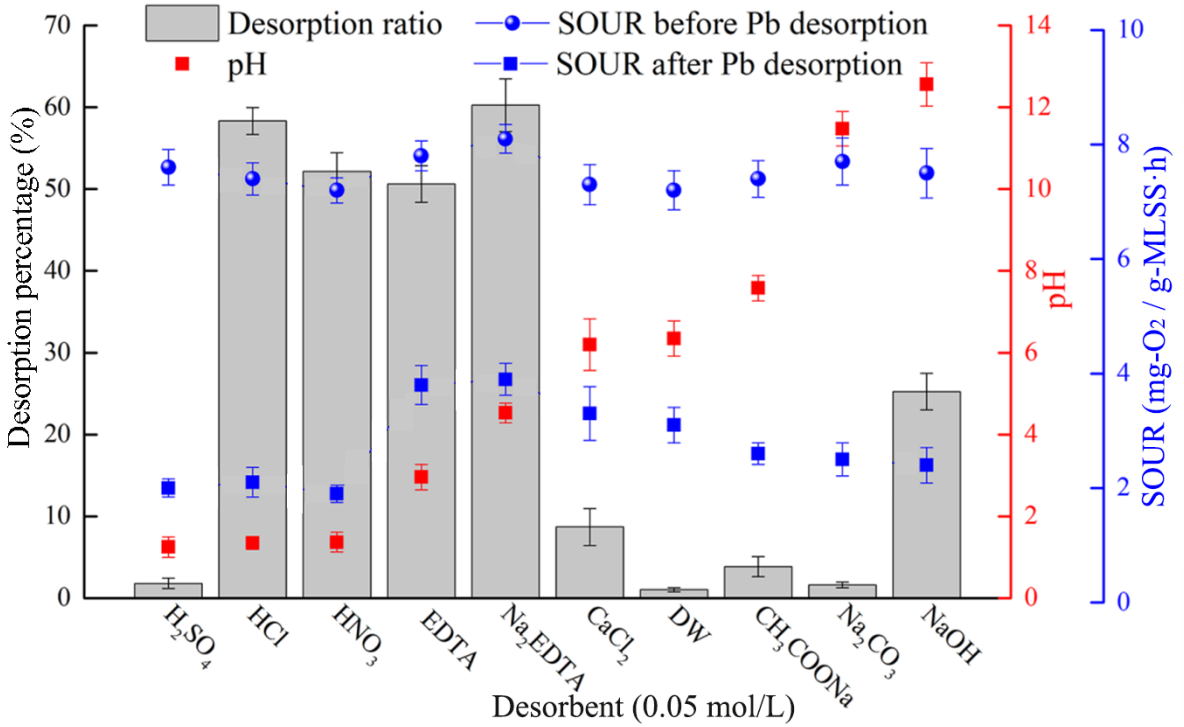

Figure 4-3. Desorption percentage of Pb from Pb-loaded algal-bacterial AGS using different desorbents (deionized water, acids (H_2SO_4, HCl and HNO_3), alkali (NaOH), salts (Na_2CO_3, $CaCl_2$, CH_3COONa), and chelating agents (EDTA and Na_2EDTA)), and the variation of SOUR of algal-bacterial AGS before and after Pb desorption. The batch experiments were conducted in 0.05 mol/L of each desorbent at the granule dosage of 1 g-MLSS/L for contacting 6 h. The data are shown as average ± standard deviation (n = 3).

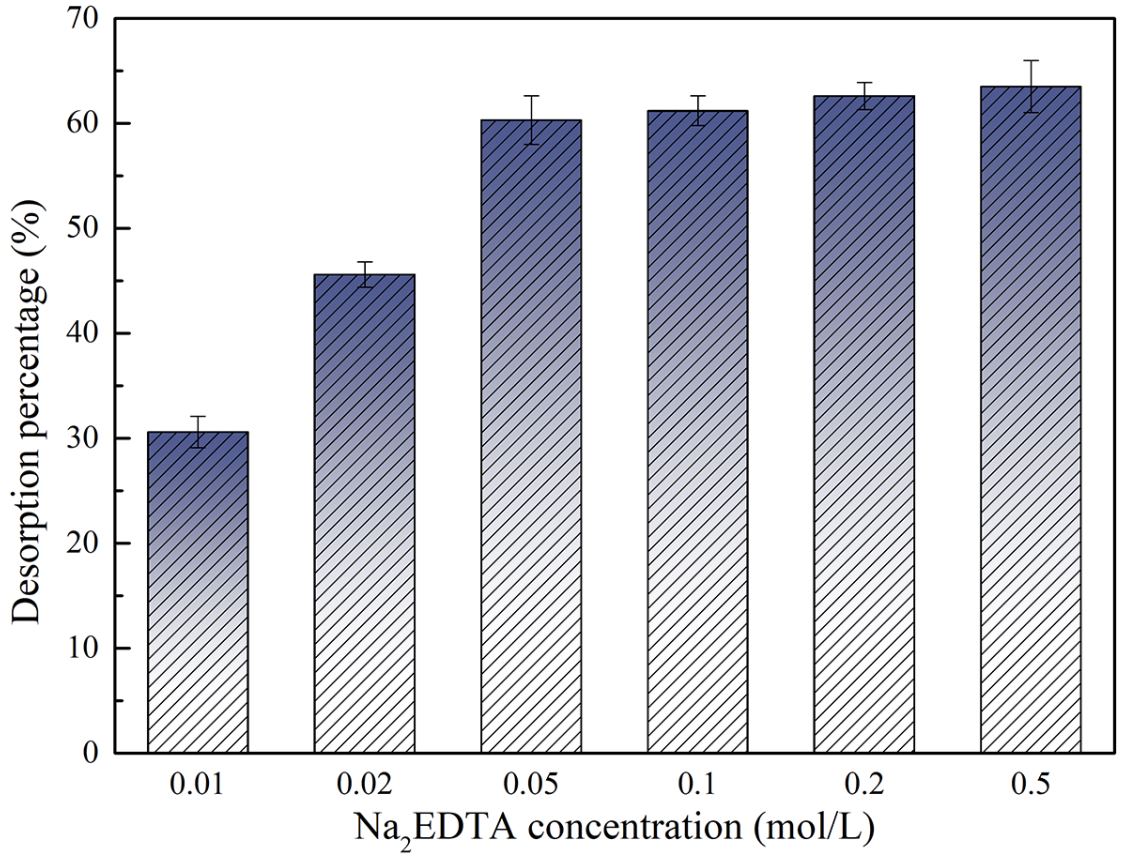

Figure 4-4. Desorption percentage of Pb from Pb-loaded algal-bacterial AGS using different concentrations of Na_2EDTA. The batch experiments were conducted in 0.01-0.5 mol/L of each desorbent at the granule dosage of 1 g-MLSS/L for contacting 6 h. The data are shown as average ± standard deviation (n = 3).

Chapter 5 Conclusions and perspectives

5.1. Conclusions

This study investigated the Pb(II) removal performance by algal-bacterial AGS with the involved mechanism being analyzed. The Pb(II) distribution and optimal desorption reagent from Pb-loaded algal-bacterial AGS were also clarified.

The biosorption performance of algal-bacterial AGS for Pb(II) was investigated with typical parameters being analyzed. Initial pH of 6.0 was determined as the optimal pH condition for Pb(II) biosorption by algal-bacterial AGS. The reaction equilibrium was achieved at about 24 h with the biosorption process better fitted the pseudo-second-order kinetic model. The biosorption isotherm better fitted the Langmuir isotherm model with a maximum adsorption capacity of 72.4 mg/g. Co-existing ions (Cr, Cu, Zn, Cd) had a slight influence on Pb(II) removal by algal-bacterial AGS. When the granule dosage was 10 g/L, the Pb(II) concentration was 0.06±0.02 mg/L which met the effluent discharge standard. Considering the quick cultivation, easy harvesting or separation, and excellent adsorption performance, the algal-bacterial AGS without pretreatment was proposed as a promising alternative to removing Pb(II) from wastewater. However, the required amount of granular dosage of 10 g/L was relatively larger for this wastewater treatment, which indicated more studies were still needed to further enhance the biosorption capacity of algal-bacterial AGS for the large-scale application of this biotechnology for Pb(II) containing wastewater treatment.

The Pb removal mechanisms by algal-bacterial AGS and the role of EPS were further clarified. Both physicochemical and biological effects were involved with electrostatic interaction, ion exchange, and bonding to functional groups orderly contributed to Pb(II) biosorption. EPS played an important role in keeping microbial activity, Pb bonding, and ion exchange in algal-bacterial AGS. Under the conditions of this experiment, 66% of the adsorbed Pb was located in the residue part (microbial cells or mineral particles) by bioaccumulation and the formation of pyromorphite precipitate ($Pb_5(PO_4)_3Cl$). This study first comprehensively revealed the Pb removal mechanisms by algal-bacterial AGS and the role of EPS in the process. Many metals including Na, Mg and Ca were released during the Pb(II) biosorption process with their active sites being occupied and most of the adsorbed Pb(II) would be in the residue part to form insoluble precipitation. The suitable separation method for adsorbed Pb need to be explored since the formation of precipitate may lower the Pb recovery efficiency.

Further, the Pb(II) distribution and the desorption from Pb-loaded algal-bacterial AGS were studied. For the adsorbed Pb in algal-bacterial AGS, 61.3% and 3.1% of them were in the organic-bound or residue fractions while 22.6% was in the mobile fraction. 60.3% of the loaded Pb could be recovered using Na_2EDTA (0.05 mol/L). Over 60% of Pb was intracellularly immobilized but the proportion for Mg or Ca was 45%, implying that the metals located in the extracellular part of algal-bacterial AGS were more likely to be mobile forms.

All the findings from this study are expected to provide the theoretical basis for the practical application of algal-bacterial AGS for cost-effective biosorption of Pb(II)-containing wastewater, contributing to mitigating the Pb-derived environmental pollution and health risk. However, the SOUR of the granules was still relatively low even though some chemicals were trying to desorb Pb(II) from the Pb-loaded granules.

5.2. Future research perspectives

Due to the complex and time-consuming cultivation processes of algal-bacterial AGS, more efforts are needed to realize its large-scale application for the treatment of Pb(II) containing wastewater as far as other HMs.

(1) Wastewater characterization: Conduct in-depth studies to characterize different types of Pb-containing wastewater to better understand how varying compositions impact the performance of the algal-bacterial system. This knowledge will help tailor the treatment approach to specific industrial effluents or contaminated sites.

(2) More studies related to microorganisms are still required to reveal the detailed mechanism in the Pb(II) adsorption process and more efficient methods to restore the granular bioactivity are needed. For the treatment of higher HMs containing wastewater or alkaline solutions, some efficient methods like domestication and pretreatment of algal-bacterial AGS are significant to investigate for the reuse of granules.

(3) The cost-efficient volume reduction methods of granules and subsequent extraction methods to separate HMs from the granular sludge residue for industrial use should be further studied considering the compact and complex physicochemical structures of granules. HM-loaded granules are still difficult to be treated for most of the adsorbed are immobile, which makes it difficult for the HMs and other resources recycling.

(4) Toxicity and ecological impacts: Assess the potential toxic effects of the treated wastewater and the generated algal-bacterial biomass. It is crucial to ensure that the treated effluent is safe for discharge into the environment and that the biomass can be safely utilized or disposed of without causing secondary pollution.

(5) The methods to keep the microbial activity and granule stability should be explored to realize the recycling use of algal-bacterial AGS for sustainable treatment of HMs containing wastewater.

References

Abbas, S.H., Ismail, I.M., Mostafa, T.M., Sulaymon, A.H., 2014. Biosorption of heavy metals: a review. J. Chem. Technol. Biotechnol. 3(4), 74-102.

Abu-Danso, E., Peraniemi, S., Leiviska, T., Bhatnagar, A., 2018. Synthesis of S-ligand tethered cellulose nanofibers for efficient removal of Pb(II) and Cd(II) ions from synthetic and industrial wastewater. Environ. Pollut. 242, 1988-1997. https://doi.org/10.1016/j.envpol.2018.07.044.

Ahmed, S., Chughtai, S., Keane, M.A., 1998. The removal of cadmium and lead from aqueous solution by ion exchange with Na-Y zeolite. Sep. Purif. Technol. 13(1), 57-64. https://doi.org/10.1016/s1383-5866(97)00063-4.

Ahmed, W., Mehmood, S., Nunez-Delgado, A., Ali, S., Qaswar, M., Shakoor, A., Mahmood, M., Chen, D., 2021. Enhanced adsorption of aqueous Pb(II) by modified biochar produced through pyrolysis of watermelon seeds. Sci. Total Environ. 784, 147136. https://doi.org/10.1016/j.scitotenv.2021.147136.

Amirnia, S., Ray, M.B., Margaritis, A., 2015. Heavy metals removal from aqueous solutions using Saccharomyces cerevisiae in a novel continuous bioreactor-biosorption system. Chem. Eng. J. 264, 863-872. https://doi.org/10.1016/j.cej.2014.12.016.

APHA, 2012. Standard methods for the examination of water and wastewater. American Public Health Association, Washington D, C., USA.

Bayuseno, A.P., Schmahl, W.W., 2011. Characterization of MSWI fly ash through mineralogy and water extraction. Resour. Conserv. Recycl. 55(5), 524-534. https://doi.org/10.1016/j.resconrec.2011.01.002.

Bazrafshan, E., Mohammadi, L., Ansari-Moghaddam, A., Mahvi, A.H., 2015. Heavy metals removal from aqueous environments by electrocoagulation process- a systematic review. J. Environ. Health Sci. Eng 13, 1-16. https://doi.org/10.1186/s40201-015-0233-8.

Cai, F., Lei, L., Li, Y., Chen, Y., 2021. A review of aerobic granular sludge (AGS) treating recalcitrant wastewater: Refractory organics removal mechanism, application and prospect. Sci. Total Environ. 782, 146852. https://doi.org/10.1016/j.scitotenv.2021.146852.

Chadha, U., Selvaraj, S.K., Thanu, S.V., Cholapadath, V., Abraham, A.M., Zaiyan, M.M., Manoharan, M., Paramsivam, V., 2022. A review of the function of using carbon nanomaterials in membrane filtration for contaminant removal from wastewater. Mater. Res. Express 9(1), 012003. https://doi.org/10.1088/2053-1591/ac48b8.

Chen, K., Zhao, Z., Yang, X., Lei, Z., Zhang, Z., Zhang, S., 2018. Desorption trials and granular stability of chromium loaded aerobic granular sludge from synthetic domestic wastewater treatment. Bioresour. Technol. Rep. 1, 9-15. https://doi.org/10.1016/j.biteb.2018.01.004.

Chen, Y., Zhang, P., Guo, J., Fang, F., Gao, X., Li, C., 2013. Functional groups characteristics of EPS in biofilm growing on different carriers. Chemosphere 92(6), 633-638. https://doi.org/10.1016/j.chemosphere.2013.01.059.

Cheng, S., Zhao, S., Guo, H., Xing, B., Liu, Y., Zhang, C., Ma, M., 2022. High-efficiency removal of lead/cadmium from wastewater by MgO modified biochar derived from crofton weed. Bioresour. Technol. 343, 126081. https://doi.org/10.1016/j.biortech.2021.126081.

Das, A., Bar, N., Das, S.K., 2020. Pb(II) adsorption from aqueous solution by nutshells, green adsorbent: Adsorption studies, regeneration studies, scale-up design, its effect on biological indicator and MLR modeling. J. Colloid Interface Sci. 580, 245-255. https://doi.org/10.1016/j.jcis.2020.07.017.

Dong, X., Zhao, Z., Yang, X., Lei, Z., Shimizu, K., Zhang, Z., Lee, D.-J., 2021. Response and recovery of mature algal-bacterial aerobic granular sludge to sudden salinity disturbance in influent wastewater: Granule characteristics and nutrients removal/accumulation. Bioresour. Technol. 321, 124492. https://doi.org/10.1016/j.biortech.2020.124492.

Ferraz, A., Teixeira, J., 1999. The use of flocculating brewer's yeast for Cr(III) and Pb(II) removal from residual wastewaters. Bioprocess Eng. 21(5), 431-437. https://doi.org/10.1007/pl00009083.

Fiol, N., Villaescusa, I., Martinez, M., Miralles, N., Poch, J., Serarols, J., 2006. Sorption of Pb(II), Ni(II), Cu(II) and Cd(II) from aqueous solution by olive stone waste. Sep. Purif. Technol. 50(1), 132-140. https://doi.org/10.1016/j.seppur.2005.11.016.

Franca, R.D.G., Pinheiro, H.M., van Loosdrecht, M.C.M., Lourenco, N.D., 2018. Stability of aerobic granules during long-term bioreactor operation. Biotechnol. Adv. 36(1), 228-246. https://doi.org/10.1016/j.biotechadv.2017.11.005.

Fu, F., Wang, Q., 2011. Removal of heavy metal ions from wastewaters: A review. J. Environ. Manage. 92(3), 407-418. https://doi.org/10.1016/j.jenvman.2010.11.011.

Goel, J., Kadirvelu, K., Rajagopal, C., Garg, V., 2005. Removal of lead(II) by adsorption using treated granular activated carbon: Batch and column studies. J. Hazard. Mater. 125(1-3), 211-220. https://doi.org/10.1016/j.jhazmat.2005.05.032.

Gu, B., Brown, G., Maya, L., Lance, M., Moyer, B., 2001. Regeneration of perchlorate (ClO_4^-)-loaded anion exchange resins by a novel tetrachloroferrate ($FeCl_4^-$) displacement technique. Environ. Sci. Technol. 35(16), 3363-3368. https://doi.org/10.1021/es010604i.

Gu, S., Boase, E.M., Lan, C.Q., 2021. Enhanced Pb(II) removal by green alga Neochloris oleoabundans cultivated in high dissolved inorganic carbon cultures. Chem. Eng. J. 416, 128983. https://doi.org/10.1016/j.cej.2021.128983.

Gu, S., Lan, C.Q., 2021. Biosorption of heavy metal ions by green alga Neochloris oleoabundans: Effects of metal ion properties and cell wall structure. J. Hazard. Mater. 418, 126336. https://doi.org/10.1016/j.jhazmat.2021.126336.

Guo, Y., Zhang, B., Feng, S., Wang, D., Li, J., Shi, W., 2022. Unveiling significance of Ca^{2+} ion for start-up of aerobic granular sludge reactor by distinguishing its effects on physicochemical property and bioactivity of sludge. Environ. Res. 212, 113299. https://doi.org/10.1016/j.envres.2022.113299.

Guyo, U., Moyo, M., 2017. Cowpea pod (Vigna unguiculata) biomass as a low-cost biosorbent for removal of Pb(II) ions from aqueous solution. Environ. Monit. Assess. 189(2), 1-13. https://doi.org/10.1007/s10661-016-5728-y.

Hammo, M.M., Akar, T., Sayin, F., Celik, S., Akar, S.T., 2021. Efficacy of green waste-derived biochar for lead removal from aqueous systems: Characterization, equilibrium, kinetic and application. J. Environ. Manage. 289, 11. https://doi.org/10.1016/j.jenvman.2021.112490.

Hoa, T.T.H., Liamleam, W., Annachhatre, A.P., 2007. Lead removal through biological sulfate reduction process. Bioresour. Technol. 98(13), 2538-2548. https://doi.org/10.1016/j.biortech.2006.09.060.

Huang, X., Wei, D., Zhang, X.W., Fan, D.W., Sun, X., Du, B., Wei, Q., 2019. Synthesis of amino-functionalized magnetic aerobic granular sludge-biochar for Pb(II) removal: Adsorption performance and mechanism studies. Sci. Total Environ. 685, 681-689. https://doi.org/10.1016/j.scitotenv.2019.05.429.

Ilmasari, D., Kamyab, H., Yuzir, A., Riyadi, F.A., Khademi, T., Al-Qaim, F.F., Kirpichnikova, I., Krishnan, S., 2022. A review of the biological treatment of leachate: Available technologies and future requirements for the circular economy implementation. Biochem. Eng. J. 187, 108605. https://doi.org/10.1016/j.bej.2022.108605.

Jaishankar, M., Tseten, T., Anbalagan, N., Mathew, B.B., Beeregowda, K.N., 2014. Toxicity, mechanism and health effects of some heavy metals. Interdisciplinary toxicology 7(2), 60.

Kim, N., Park, M., Park, D., 2015. A new efficient forest biowaste as biosorbent for removal of cationic heavy metals. Bioresour. Technol. 175, 629-632. https://doi.org/10.1016/j.biortech.2014.10.092.

Kipigroch, K., 2020. The use of algae to remove zinc and lead from industrial wastewater. Desalin. Water Treat. 199, 323-330. https://doi.org/10.5004/dwt.2020.26341.

Klik, B., Gusiatin, Z.M., Kulikowska, D., 2021. A holistic approach to remediation of soil contaminated with Cu, Pb and Zn with sewage sludge-derived washing agents and synthetic chelator. J. Cleaner Prod. 311, 127664. https://doi.org/10.1016/j.jclepro.2021.127664.

Kumar, B., Smita, K., Sanchez, E., Stael, C., Cumbal, L., 2016. Andean Sacha inchi (Plukenetia volubilis L.) shell biomass as new biosorbents for Pb^{2+} and Cu^{2+} ions. Ecol. Eng. 93, 152-158. https://doi.org/10.1016/j.ecoleng.2016.05.034.

Kumar, K.S., Dahms, H.U., Won, E.J., Lee, J.S., Shin, K.H., 2015. Microalgae - A promising tool for heavy metal remediation. Ecotox. Environ. Safe. 113, 329-352. https://doi.org/10.1016/j.ecoenv.2014.12.019.

Li, N., Wei, D., Wang, S., Hu, L., Xu, W., Du, B., Wei, Q., 2017a. Comparative study of the role of extracellular polymeric substances in biosorption of Ni(II) onto aerobic/anaerobic granular sludge. J. Colloid Interface Sci. 490, 754-761. https://doi.org/10.1016/j.jcis.2016.12.006.

Li, Y., Song, S., Xia, L., Yin, H., Garcia Meza, J.V., Ju, W., 2019. Enhanced Pb(II) removal by algal-based biosorbent cultivated in high-phosphorus cultures. Chem. Eng. J. 361, 167-179. https://doi.org/10.1016/j.cej.2018.12.070.

Li, Y., Styczynski, J., Huang, Y.K., Xu, Z.H., McCutcheon, J., Li, B.K., 2017b. Energy-positive wastewater treatment and desalination in an integrated microbial desalination cell (MDC)-microbial electrolysis cell (MEC). J. Power Sources 356, 529-538. https://doi.org/10.1016/j.jpowsour.2017.01.069.

Liao, T., Xi, Y., zhang, L., Li, J., Cui, K., 2021. Removal of toxic arsenic (As(III)) from industrial wastewater by ultrasonic enhanced zero-valent lead combined with $CuSO_4$. J. Hazard. Mater. 408, 124464. https://doi.org/10.1016/j.jhazmat.2020.124464.

Liu, J., Zhou, J., Wu, Z.H., Tian, X., An, X.Y., Zhang, Y., Zhang, G.S., Deng, F.X., Meng, X.L., Qu, J.H., 2022. Concurrent elimination and stepwise recovery of Pb(II) and bisphenol A from water using beta-cyclodextrin modified magnetic cellulose: adsorption performance and mechanism investigation. J. Hazard. Mater. 432, 128758. https://doi.org/10.1016/j.jhazmat.2022.128758.

Liu, L., Huang, Y., Zhang, S., Gong, Y., Su, Y., Cao, J., Hu, H., 2019a. Adsorption characteristics and mechanism of Pb(II) by agricultural waste-derived biochars produced from a pilot-scale pyrolysis system. Waste Manage. 100, 287-295. https://doi.org/10.1016/j.wasman.2019.08.021.

Liu, L., Sheng, G., Liu, Z., Li, W., Zeng, R.J., Lee, D., Liu, J., Yu, H., 2010. Characterization of multiporous structure and oxygen transfer inside aerobic granules with the percolation model. Environ. Sci. Technol. 44(22), 8535-8540. https://doi.org/10.1021/es102437a.

Liu, L.Q., Huang, Y.J., Zhang, S.P., Gong, Y., Su, Y.H., Cao, J.H., Hu, H.J., 2019b. Adsorption characteristics and mechanism of Pb(II) by agricultural waste-derived biochars produced from a pilot-scale pyrolysis system. Waste Manage. 100, 287-295. https://doi.org/10.1016/j.wasman.2019.08.021.

Lyu, F., Niu, S., Wang, L., Liu, R., Sun, W., He, D., 2021. Efficient removal of Pb(II) ions from aqueous solution by modified red mud. J. Hazard. Mater. 406, 124678. https://doi.org/10.1016/j.jhazmat.2020.124678.

Mal, J., Sinharoy, A., Lens, P.N.L., 2021. Simultaneous removal of lead and selenium through biomineralization as lead selenide by anaerobic granular sludge. J. Hazard. Mater. 420, 126663. https://doi.org/10.1016/j.jhazmat.2021.126663.

Meng, F., Xi, L., Liu, D., Huang, W., Lei, Z., Zhang, Z., Huang, W., 2019. Effects of light intensity on oxygen distribution, lipid production and biological community of algal-bacterial granules in photo-sequencing batch reactors. Bioresour. Technol. 272, 473-481. https://doi.org/10.1016/j.biortech.2018.10.059.

Meng, L., Li, Z., Liu, L., Chen, X., Wu, J., Li, W., Zhang, X., Dong, M., 2020. Lead removal from water by a newly isolated Geotrichum candidum LG-8 from Tibet kefir milk and its

mechanism. Chemosphere 259, 127507. https://doi.org/10.1016/j.chemosphere.2020.127507.

Mohapatra, R.K., Parhi, P.K., Pandey, S., Bindhani, B.K., Thatoi, H., Panda, C.R., 2019. Active and passive biosorption of Pb(II)using live and dead biomass of marine bacterium Bacillus xiamenensis PbRPSD202: Kinetics and isotherm studies. J. Environ. Manage. 247, 121-134. https://doi.org/10.1016/j.jenvman.2019.06.073.

Nair, A., Juwarkar, A.A., Devotta, S., 2008. Study of speciation of metals in an industrial sludge and evaluation of metal chelators for their removal. J. Hazard. Mater. 152(2), 545-553. https://doi.org/10.1016/j.jhazmat.2007.07.054.

Nassar, N.N., 2010. Rapid removal and recovery of Pb(II) from wastewater by magnetic nanoadsorbents. J. Hazard. Mater. 184(1-3), 538-546. https://doi.org/10.1016/j.jhazmat.2010.08.069.

Nicomel, N.R., Otero-Gonzalez, L., Arashiro, L., Garfi, M., Ferrer, I., Van Der Voort, P., Verbeken, K., Hennebel, T., Du Laing, G., 2020. Microalgae: a sustainable adsorbent with high potential for upconcentration of indium(iii) from liquid process and waste streams. Green Chem. 22(6), 1985-1995. https://doi.org/10.1039/c9gc03073e.

Pagliaccia, B., Carretti, E., Severi, M., Berti, D., Lubello, C., Lotti, T., 2022. Heavy metal biosorption by extracellular polymeric substances (EPS) recovered from anammox granular sludge. J. Hazard. Mater. 424, 126661. https://doi.org/10.1016/j.jhazmat.2021.126661.

Priyadharshini, S.D., Babu, P.S., Manikandan, S., Subbaiya, R., Govarthanan, M., Karmegam, N., 2021. Phycoremediation of wastewater for pollutant removal: A green approach to environmental protection and long-term remediation. Environ. Pollut. 290, 117989. https://doi.org/10.1016/j.envpol.2021.117989.

Qin, H., Hu, T., Zhai, Y., Lu, N., Aliyeva, J., 2020. The improved methods of heavy metals removal by biosorbents: A review. Environ. Pollut. 258, 113777. https://doi.org/10.1016/j.envpol.2019.113777.

Salahandish, R., Ghaffarinejad, A., Norouzbeigi, R., 2016. Rapid and efficient lead(II) ion removal from aqueous solutions using Malva sylvestris flower as a green biosorbent. Anal. Methods 8(11), 2515-2525. https://doi.org/10.1039/c5ay02681d.

Sanchez-Sanchez, C., Baquerizo, G., Moreno-Rodriguez, E., 2023. Analysing the influence of operating conditions on the performance of algal-bacterial granular sludge processes for wastewater treatment: A review. Water Environ. J. https://doi.org/10.1111/wej.12873.

Saravanan, A., Kumar, P.S., Varjani, S., Jeevanantham, S., Yaashikaa, P.R., Thamarai, P., Abirami, B., George, C.S., 2021. A review on algal-bacterial symbiotic system for effective treatment of wastewater. Chemosphere 271, 129540. https://doi.org/10.1016/j.chemosphere.2021.129540.

Schwantes, D., Goncalves, A.C., Jr., Coelho, G.F., Campagnolo, M.A., Dragunski, D.C., Teixeira Tarley, C.R., Miola, A.J., Volz Leismann, E.A., 2016. Chemical Modifications

of Cassava Peel as Adsorbent Material for Metals Ions from Wastewater. J. Chem. https://doi.org/10.1155/2016/3694174.

Shen, L., Wang, J., Li, Z., Fan, L., Chen, R., Wu, X., Li, J., Zeng, W., 2020. A high-efficiency Fe_2O_3@Microalgae composite for heavy metal removal from aqueous solution. J. Water Process. Eng. 33, 101026. https://doi.org/10.1016/j.jwpe.2019.101026.

Sheng, G., Yu, H., Li, X., 2010. Extracellular polymeric substances (EPS) of microbial aggregates in biological wastewater treatment systems: A review. Biotechnol. Adv. 28(6), 882-894. https://doi.org/10.1016/j.biotechadv.2010.08.001.

Shi, L., Wei, D., Ngo, H.H., Guo, W., Du, B., Wei, Q., 2015. Application of anaerobic granular sludge for competitive biosorption of methylene blue and Pb(II): Fluorescence and response surface methodology. Bioresour. Technol. 194, 297-304. https://doi.org/10.1016/j.biortech.2015.07.029.

Son, E.B., Poo, K.M., Chang, J.S., Chae, K.J., 2018. Heavy metal removal from aqueous solutions using engineered magnetic biochars derived from waste marine macro-algal biomass. Sci. Total Environ. 615, 161-168. https://doi.org/10.1016/j.scitotenv.2017.09.171.

Taki, K., Gogoi, A., Mazumder, P., Bhattacharya, S.S., Kumar, M., 2019. Efficacy of vermitechnology integration with upflow anaerobic ludge Blanket (UASB) and activated sludge for metal stabilization: A compliance study on fractionation and biosorption. J. Environ. Manage. 236, 603-612. https://doi.org/10.1016/j.jenvman.2019.01.006.

Tan, Y., Wan, X., Zhou, T., Wang, L., Yin, X., Ma, A., Wang, N., 2022. Novel Zn-Fe engineered kiwi branch biochar for the removal of Pb(II) from aqueous solution. J. Hazard. Mater. 424, 127349. https://doi.org/10.1016/j.jhazmat.2021.127349.

Tessier, A., Campbell, P.G.C., Bisson, M., 1979. Sequential extraction procedure for the speciation of particulate trace metals. Anal. Chem. 51(7), 844-851. https://doi.org/10.1021/ac50043a017.

Vardhan, K.H., Kumar, P.S., Panda, R.C., 2019. A review on heavy metal pollution, toxicity and remedial measures: Current trends and future perspectives. J. Mol. Liq. 290, 111197. https://doi.org/10.1016/j.molliq.2019.111197.

Wang, C., Wei, W., Zhang, Y., Dai, X., Ni, B., 2022a. Different sizes of polystyrene microplastics induced distinct microbial responses of anaerobic granular sludge. Water Res. 220, 118607. https://doi.org/10.1016/j.watres.2022.118607.

Wang, J., Li, Q., Li, M., Chen, T., Zhou, Y., Yue, Z., 2014. Competitive adsorption of heavy metal by extracellular polymeric substances (EPS) extracted from sulfate reducing bacteria. Bioresour. Technol. 163, 374-376. https://doi.org/10.1016/j.biortech.2014.04.073.

Wang, L., Liu, X., Lee, D., Tay, J., Zhang, Y., Wan, C., Chen, X., 2018. Recent advances on biosorption by aerobic granular sludge. J. Hazard. Mater. 357, 253-270. https://doi.org/10.1016/j.jhazmat.2018.06.010.

Wang, Q., Shen, Q., Wang, J., Zhao, J., Zhang, Z., Lei, Z., Yuan, T., Shimizu, K., Liu, Y., Lee, D.-J., 2022b. Insight into the rapid biogranulation for suspended single-cell microalgae harvesting in wastewater treatment systems: Focus on the role of extracellular polymeric substances. Chem. Eng. J. 430, 132631. https://doi.org/10.1016/j.cej.2021.132631.

Wang, Q., Zheng, C., Shen, Z., Lu, Q., He, C., Zhang, T.C., Liu, J., 2019. Polyethyleneimine and carbon disulfide co-modified alkaline lignin for removal of Pb^{2+} ions from water. Chem. Eng. J. 359, 265-274. https://doi.org/10.1016/j.cej.2018.11.130.

Wang, S., Tang, Y., Chen, C., Wu, J., Huang, Z., Mo, Y., Zhang, K., Chen, J., 2015. Regeneration of magnetic biochar derived from eucalyptus leaf residue for lead(II) removal. Bioresour. Technol. 186, 360-364. https://doi.org/10.1016/j.biortech.2015.03.139.

Wang, X., Song, R., Teng, S., Gao, M., Ni, J., Liu, F., Wang, S., Gao, B., 2010. Characteristics and mechanisms of Cu(II) biosorption by disintegrated aerobic granules. J. Hazard. Mater. 179(1-3), 431-437. https://doi.org/10.1016/j.jhazmat.2010.03.022.

Wei, D., Li, M., Wang, X., Han, F., Li, L., Guo, J., Ai, L., Fang, L., Liu, L., Du, B., Wei, Q., 2016. Extracellular polymeric substances for Zn (II) binding during its sorption process onto aerobic granular sludge. J. Hazard. Mater. 301, 407-415. https://doi.org/10.1016/j.jhazmat.2015.09.018.

World Health Organization (WHO), 2021. A global overview of national regulations and standards for drinking-water quality.

Wu, J., Zhang, H., He, P.J., Yao, Q., Shao, L.M., 2010. Cr(VI) removal from aqueous solution by dried activated sludge biomass. J. Hazard. Mater. 176(1-3), 697-703. https://doi.org/10.1016/j.jhazmat.2009.11.088.

Xi, Y., Zou, J., Luo, Y., Li, J., Li, X., Liao, T., Zhang, L., Wang, C., Lin, G., 2019. Performance and mechanism of arsenic removal in waste acid by combination of $CuSO_4$ and zero-valent iron. Chem. Eng. J. 375, 9. https://doi.org/10.1016/j.cej.2019.121928.

Xiang, H., Min, X., Tang, C.-J., Sillanpaa, M., Zhao, F., 2022. Recent advances in membrane filtration for heavy metal removal from wastewater: A mini review. J. Water Process. Eng. 49, 103023. https://doi.org/10.1016/j.jwpe.2022.103023.

Xiong, W., Wang, S., Jin, Y., Wu, Z., Liu, D., Su, H., 2023. Insights into nitrogen and phosphorus metabolic mechanisms of algal-bacterial aerobic granular sludge via metagenomics: Performance, microbial community and functional genes. Bioresour. Technol. 369, 128442. https://doi.org/10.1016/j.biortech.2022.128442.

Xiong, Y., Liu, Y., 2013. Importance of extracellular proteins in maintaining structural integrity of aerobic granules. Colloid Surf. B-Biointerfaces 112, 435-440. https://doi.org/10.1016/j.colsurfb.2013.07.060.

Xu, H., Liu, Y., 2008. Mechanisms of Cd^{2+}, Cu^{2+} and Ni^{2+} biosorption by aerobic granules. Sep. Purif. Technol. 58(3), 400-411. https://doi.org/10.1016/j.seppur.2007.05.018.

Xu, R., Tang, C., Liu, M., 2020a. A novel nitrified aerobic granular sludge biosorbent for Pb(II) removal: behaviors and mechanisms. J. Dispersion Sci. Technol. 41(14), 2223-2231. https://doi.org/10.1080/01932691.2019.1656641.

Xu, X., Hao, R., Xu, H., Lu, A., 2020b. Removal mechanism of Pb(II) by Penicillium polonicum: immobilization, adsorption, and bioaccumulation. Sci. Rep. 10(1), 9079. https://doi.org/10.1038/s41598-020-66025-6.

Xu, Y.-N., Chen, Y., 2020. Advances in heavy metal removal by sulfate-reducing bacteria. Water Sci. Technol. 81(9), 1797-1827. https://doi.org/10.2166/wst.2020.227.

Yang, X., Nguyen, V.B., Zhao, Z., Wu, Y., Lei, Z., Zhang, Z., Le, X.S., Lu, H., 2022. Changes of distribution and chemical speciation of metals in hexavalent chromium loaded algal-bacterial aerobic granular sludge before and after hydrothermal treatment. Bioresour. Technol. 355, 9079. https://doi.org/10.1016/j.biortech.2022.127229.

Yang, X., Zhao, Z., Van Nguyen, B., Hirayama, S., Tian, C., Lei, Z., Shimizu, K., Zhang, Z., 2021a. Cr(VI) bioremediation by active algal-bacterial aerobic granular sludge: Importance of microbial viability, contribution of microalgae and fractionation of loaded Cr. J. Hazard. Mater. 418, 126342. https://doi.org/10.1016/j.jhazmat.2021.126342.

Yang, X., Zhao, Z., Yu, Y., Shimizu, K., Zhang, Z., Lei, Z., Lee, D.-J., 2020. Enhanced biosorption of Cr(VI) from synthetic wastewater using algal-bacterial aerobic granular sludge: Batch experiments, kinetics and mechanisms. Sep. Purif. Technol. 251, 117323. https://doi.org/10.1016/j.seppur.2020.117323.

Yang, X., Zhao, Z., Zhang, G., Hirayama, S., Nguyen, B.V., Lei, Z., Shimizu, K., Zhang, Z., 2021b. Insight into Cr(VI) biosorption onto algal-bacterial granular sludge: Cr(VI) bioreduction and its intracellular accumulation in addition to the effects of environmental factors. J. Hazard. Mater. 414, 125479. https://doi.org/10.1016/j.jhazmat.2021.125479.

Yetis, U., Dolek, A., Dilek, F., Ozcengiz, G., 2000. The removal of Pb(II) by Phanerochaete chrysosporium. Water Res. 34(16), 4090-4100. https://doi.org/10.1016/s0043-1354(00)00155-x.

Yuan, T., Xu, J., Wang, Z., Lei, Z., Kato, M., Shimizu, K., Zhang, Z., 2023. Efficient removal of molybdate from groundwater with visible color changes using wasted aerobic granular sludge. Sep. Purif. Technol. 317, 123849. https://doi.org/10.1016/j.seppur.2023.123849.

Zeng, Q., Huang, Y., Huang, L., Li, S., Hu, L., Xiong, D., Zhong, H., He, Z., 2020. A novel composite of SiO_2 decorated with nano ferrous oxalate (SDNF) for efficient and highly selective removal of Pb^{2+} from aqueous solutions. J. Hazard. Mater. 391, 122193. https://doi.org/10.1016/j.jhazmat.2020.122193.

Zeng, X., Zeng, Z., Wang, Q., Liang, W., Guo, Y., Huo, X., 2022. Alterations of the gut microbiota and metabolomics in children with e-waste lead exposure. J. Hazard. Mater. 434, 128842. https://doi.org/10.1016/j.jhazmat.2022.128842.

Zhang, B., Guo, Y., Lens, P.N.L., Zhang, Z., Shi, W., Cui, F., Tay, J.H., 2019. Effect of light intensity on the characteristics of algal-bacterial granular sludge and the role of N-acyl-

homoserine lactone in the granulation. Sci. Total Environ. 659, 372-383. https://doi.org/10.1016/j.scitotenv.2018.12.250.

Zhang, B., Lens, P.N.L., Shi, W., Zhang, R., Zhang, Z., Guo, Y., Bao, X., Cui, F., 2018. Enhancement of aerobic granulation and nutrient removal by an algal-bacterial consortium in a lab-scale photobioreactor. Chem. Eng. J. 334, 2373-2382. https://doi.org/10.1016/j.cej.2017.11.151.

Zhang, B., Li, W., Guo, Y., Zhang, Z., Shi, W., Cui, F., Lens, P.N.L., Tay, J.H., 2020a. Microalgal-bacterial consortia: From interspecies interactions to biotechnological applications. Renew. Sust. Energ. Rev. 118, 109563. https://doi.org/10.1016/j.rser.2019.109563.

Zhang, K., Xue, Y., Zhang, J., Hu, X., 2020b. Removal of lead from acidic wastewater by bio-mineralized bacteria with pH self-regulation. Chemosphere 241, 125041. https://doi.org/10.1016/j.chemosphere.2019.125041.

Zhang, L., Lin, X.J., Wang, J.T., Jiang, F., Wei, L., Chen, G.H., Hao, X.D., 2016. Effects of lead and mercury on sulfate-reducing bacterial activity in a biological process for flue gas desulfurization wastewater treatment. Sci. Rep. 6, 1-10. https://doi.org/10.1038/srep30455.

Zhao, D., Cheah, W.Y., Lai, S.H., Ng, E.-P., Khoo, K.S., Show, P.L., Ling, T.C., 2023. Symbiosis of microalgae and bacteria consortium for heavy metal remediation in wastewater. J. Environ. Chem. Eng. 11(3), 109943. https://doi.org/10.1016/j.jece.2023.109943.

Zhao, W., Zhu, G., Daugulis, A.J., Chen, Q., Ma, H., Zheng, P., Liang, J., Ma, X., 2020. Removal and biomineralization of Pb^{2+} in water by fungus Phanerochaete chrysoporium. J. Cleaner Prod. 260, 120980. https://doi.org/10.1016/j.jclepro.2020.120980.

Zhou, Y., Zhang, Z.Q., Zhang, J., Xia, S.Q., 2016. Understanding key constituents and feature of the biopolymer in activated sludge responsible for binding heavy metals. Chem. Eng. J. 304, 527-532. https://doi.org/10.1016/j.cej.2016.06.115.

Zhu, L., Lv, M., Dai, X., Yu, Y., Qi, H., Xu, X., 2012. Role and significance of extracellular polymeric substances on the property of aerobic granule. Bioresour. Technol. 107, 46-54. https://doi.org/10.1016/j.biortech.2011.12.008.

Acknowledgements

First of all, I would like to express my sincere appreciation for my supervisor Prof. Dr. Zhenya Zhang. Whenever I have any trouble during my study and life, you show me the way and give selfless help. I would like to appreciate my co-supervisor Asst. Prof. Dr. Tian Yuan and Assoc. Prof. Dr. Zhongfang Lei. Without your patient instruction and careful revision, I couldn't finish the papers and the final thesis. I would like to express thanks for the guidance and help from Prof. Dr. Kazuya Shimizu.

I would like to thank for the thesis committee members, Prof. Dr. Zhenya Zhang, Asst. Prof. Dr. Tian Yuan, Assoc. Prof. Dr. Zhongfang Lei, Prof. Dr. Kazuya Shimizu and Asst. Prof. Dr. Tomoyuki Yokoi. It is deeply appreciated for your valuable comments and suggestions, which makes the thesis improved a lot.

I would like to appreciate all the guys who help me during my doctoral study and life in Tsukuba. Firstly, many thanks to Dr. Yong Jiang and Dr. Ying Wang, who help me whenever I have trouble. Thanks for your kind help and support from the heart. Secondly, thanks for the seniors of our lab, Dr. Ziwen Zhao, Dr. Xiaojing Yang, Dr. Jiamin Zhao, Dr. Tingting Hou, Dr. Qian Wang, Dr. Lanting Wang and others, who give me many help and guidance. Thirdly, thanks for the help and suggestions from our lab guys, Mr. Hanxiao Wang, Mr. Chi Zhang, Mr. Yang Shi, Dr. Ji Zhang, Dr. Hanchen Miao and others, who give care during the study and life. Thanks for the help from many seniors and friends for many years at home and abroad.

Thanks for the financial support from the China Scholarship Council (CSC) during my study at University of Tsukuba.

Thanks for the support and understanding from my beloved parents and elder sister. I would like to express my deep gratitude and you make me strong.

Heart's desire, omnipotent!

List of publications

- First author papers

1. **Zhiwei Wang**, Hanxiao Wang, Qi Nie, Yi Ding, Zhongfang Lei, Zhenya Zhang, Kazuya Shimizu, Tian Yuan, Pb(II) bioremediation using fresh algal-bacterial aerobic granular sludge and its underlying mechanisms highlighting the role of extracellular polymeric substances, ***Journal of Hazardous Materials***, Vol. 444, No. 130452, 2023.
2. **Zhiwei Wang**, Zhenya Zhang, Tian Yuan, Kazuya Shimizu, Ding Wang, Daijiang Luo, Daoxiang Wang, Juanjian Ru, Direct electroseparation of zinc from zinc sulfide in eco-friendly deep eutectic solvent: Highlighting the role of malonic acid, ***Separation and Purification Technology***, Vol. 306, No. 122686, 2023.
3. **Zhiwei Wang**, Zhi Li, Jiaojiao Bu, Juanjian Ru, Yixin Hua, Ding Wang, One-step direct desulfurization of cuprous sulfide for copper recovery via electrolysis in deep eutectic solvent, ***Separation and Purification Technology,*** Vol. 303, No. 122133, 2022.
4. **Zhiwei Wang**, Mingqiang Cheng, Jiaojiao Bu, Lei Cheng, Juanjian Ru, Yixin Hua, Ding Wang, Understanding the electrochemical behavior of Sn(II) in choline chloride-ethylene glycol deep eutectic solvent for tin powders preparation, ***Advanced Powder Technology***, Vol. 33, No. 103670, 2022.
5. **Zhiwei Wang**, Teng Wu, Xiao Geng, Juanjian Ru, Yixin Hua, Jiaojiao Bu, Yu Xue, Ding Wang, The role of electrolyte ratio in electrodeposition of nanoscale Fe-Cr alloy from choline chloride-ethylene glycol ionic liquid: A suitable layer for corrosion resistance, ***Journal of Molecular Liquids***, Vol. 346, No. 117059, 2022.
6. **Zhiwei Wang**, Juanjian Ru, Yixin Hua, Jiaojiao Bu, Xiao Geng, Wenwen Zhang, Electrodeposition of Sn powders with pyramid chain and dendrite structures in deep eutectic solvent: roles of current density and $SnCl_2$ concentration, ***Journal of Solid State Electrochemistry***, Vol. 25, pp. 1111-1120, 2021.
7. **Zhiwei Wang**, Teng Wu, Juanjian Ru, Yixin Hua, Jiaojiao Bu, Ding Wang, Eco-friendly preparation of nanocrystalline Fe-Cr alloy coating by electrodeposition in deep eutectic solvent without any additives for anti-corrosion, ***Surface and Coatings Technology***, Vol. 406, No. 126636, 2021.
8. **Zhiwei Wang**, Juanjian Ru, Yixin Hua, Ding Wang, Jiaojiao Bu, Morphology-controlled preparation of Sn powders by electrodeposition in deep eutectic solvent as anodes for lithium ion batteries, ***Journal of the Electrochemical Society***, Vol. 167, No. 082504, 2020.
9. **Zhiwei Wang**, Juanjian Ru, Jiaojiao Bu, Yixin Hua, Yuan Zhang, Cunying Xu, Direct electrochemical desulfurization of solid Sb_2S_3 to antimony powders in deep eutectic solvent, ***Journal of the Electrochemical Society***, Vol. 166, pp. D747-D754, 2019.

- Co-author papers

10. Tian Yuan, Jing Xu, **Zhiwei Wang**, Zhongfang Lei, Masashi Kato, Kazuya Shimizu,

Zhenya Zhang, Efficient removal of molybdate from groundwater with visible color changes using wasted aerobic granular sludge, ***Separation and Purification Technology***, Vol. 317, No. 123849, 2023.

11. Lanting Wang, Tianxiao Liu, Jing Xu, **Zhiwei Wang**, Zhongfang Lei, Kazuya Shimizu, Zhenya Zhang, Tian Yuan*, Enhanced economic benefit of recycling Fe_3O_4 for promotion of volatile fatty acids production in anaerobic fermentation of food waste, ***Bioresource Technology***, Vol. 369, No. 128428, 2023.
12. Hanxiao Wang, Tongtong Liu, Yi Ding, **Zhiwei Wang**, Zhenya Zhang, Zhongfang Lei, Kazuya Shimizu, Tian Yuan, Enhanced performance of algal-bacterial aerobic granular sludge in comparison to bacterial aerobic granular sludge for treating surfactant-containing wastewater, ***Bioresource Technology Reports***, Vol. 22, No., 101462 2023.
13. Chengcheng Fu, Juanjian Ru, Yixin Hua, Yu Xue, Jiaojiao Bu, **Zhiwei Wang**, Electrochemical separation of high-purity Sb from Pb-containing Sb aloy in choline chloride-ethylene glycol deep eutectic solvent, ***JOM***, Vol. 74, pp. 915–923, 2022.
14. Jiaojiao Bu, Juanjian Ru, Yixin Hua, **Zhiwei Wang**, Yuan Zhang, Xiao Geng, Wenwen Zhang, Electrochemical behavior of Sb(III)/Sb during the preparation of Sb particles in deep eutectic solvent, ***Ionics***, Vol. 27, pp. 3119-3127, 2021.
15. Yu Xue, Yixin Hua, Juanjian Ru, Chengcheng Fu, **Zhiwei Wang**, Jiaojiao Bu, High-efficiency separation of Ni from Cu-Ni alloy by electrorefining in choline chloride-ethylene glycol deep eutectic solvent, ***Advanced Powder Technology***, Vol. 32, pp. 2791-2797, 2021.
16. Yuan Zhang, Juanjian Ru, Yixin Hua, Ping Huang, Jiaojiao Bu, **Zhiwei Wang**, Facile and controllable synthesis of NiS_2 nanospheres in deep eutectic solvent, ***Materials Letters*****,** Vol. 283, No. 128742, 2021.
17. JiaoJiao Bu, Juanjian Ru, **Zhiwei Wang**, Yixin Hua, Cunying Xu, Yuan Zhang, Controllable preparation of antimony powders by electrodeposition in choline chloride-ethylene glycol, ***Advanced Powder Technology***, Vol. 30, pp. 2859-2867, 2019.
18. Juanjian Ru, Jiaojiao Bu, **Zhiwei Wang**, Yixin Hua, Ding Wang, Eco-friendly and facile electrochemical synthesis of sub-micrometer lead powders in deep eutectic solvents using galena as a raw material, ***Journal of Applied Electrochemistry***, Vol. 49, pp. 369-377, 2019.
19. Juanjian Ru, **Zhiwei Wang**, Jiaojiao Bu, Yixin Hua, Ding Wang, One-step electrochemical preparation of lead powders and sulfur nanoparticles from solid lead sulfide in deep eutectic solvents without SO_2 Gas, ***Journal of the Electrochemical Society*****,** Vol. 165, pp. 482-487, 2018.